NASA Contractor Report 181690

ICASE REPORT NO. 88-43

ICASE

ON THE GENERATION OF MEAN FLOWS BY THE INTERACTION OF GÖRTLER VORTICES AND TOLLMIEN-SCHLICHTING WAVES IN CURVED CHANNEL FLOWS

Andrew P. Bassom

Philip Hall

Contract Nos. NAS1-18107 and NAS1-18605
July 1988

INSTITUTE FOR COMPUTER APPLICATIONS IN SCIENCE AND ENGINEERING
NASA Langley Research Center, Hampton, Virginia 23665

Operated by the Universities Space Research Association

National Aeronautics and
Space Administration

Langley Research Center
Hampton, Virginia 23665

ON THE GENERATION OF MEAN FLOWS BY THE INTERACTION OF GÖRTLER VORTICES AND TOLLMIEN-SCHLICHTING WAVES IN CURVED CHANNEL FLOWS

Andrew P. Bassom and Philip Hall

Department of Mathematics,
North Park Road,
University of Exeter,
EXETER, DEVON
U.K.

ABSTRACT

There are many fluid flows where the onset of transition can be caused by different instability mechanisms which compete in the nonlinear regime. Here the interaction of a centrifugal instability mechanism with the viscous mechanism which causes Tollmien-Schlichting waves is discussed. The interaction between these modes can be strong enough to drive the mean state; here the interaction is investigated in the context of curved channel flows so as to avoid difficulties associated with boundary layer growth. Essentially it is found that the mean state adjusts itself so that any modes present are neutrally stable even at finite amplitude. In the first instance, the mean state driven by a vortex of short wavelength in the absence of a Tollmien-Schlichting wave is considered. It is shown that for a given channel curvature and vortex wavelength there is an upper limit to the mass flow rate which the channel can support as the pressure gradient is increased. When Tollmien-Schlichting waves are present then the nonlinear differential equation to determine the mean state is modified. At sufficiently high Tollmien-Schlichting amplitudes it is found that the vortex flows are destroyed, but there is a range of amplitudes where a fully nonlinear mixed vortex-wave state exists and indeed drives a mean state having little similarity with the flow which occurs without the instability modes. The vortex and Tollmien-Schlichting wave structure in the nonlinear regime has viscous wall layers and internal shear layers; the thickness of the internal layers is found to be a function of the Tollmien-Schlichting wave amplitude.

This research was supported by the National Aeronautics and Space Administration under NASA Contract Nos. NAS1-18107 and NAS1-18605 while the second author was in residence at the Institute for Computer Applications in Science and Engineering (ICASE), NASA Langley Research Center, Hampton, VA 23665.

§1. Introduction.

Our concern is with the strongly nonlinear interaction of large amplitude Tollmien-Schlichting waves and Görtler vortices in curved channel flows. Interaction problems of this type are relevant to many flows of practical importance where viscosity and centrifugal effects combine to stimulate travelling wave disturbances and stationary vortices. The most obvious examples are the flow driven by a steady pressure gradient in a curved duct and the flow over a laminar flow aerofoil, see Harvey & Pride (**1**). In the latter problem, a question of fundamental importance is whether the presence of finite amplitude Görtler vortices and Tollmien-Schlichting waves and their consequent interaction cause the premature onset of transition.

Here, because of the difficulties associated with boundary layer growth, we concentrate on fully developed curved channel flows driven by azimuthal pressure gradients. We shall, however, indicate the probable relevance of our calculations to the external flow situation. The interaction which we consider is strong enough for the Tollmien-Schlichting waves (hereafter referred to as TS waves) to have an O(1) effect on the steady vortex flow which exists in the absence of the waves. Likewise this O(1) correction to the vortex state has an O(1) effect back on the wave so that the vortex and the TS states are strongly coupled. Remarkably this strong interaction occurs at extremely small TS amplitudes; it is the large inertial effects associated with both the TS wave and Görtler vortex which generate this large response.

The basis for the expansion procedure to describe the interaction is that given by Hall & Lakin (**2**) for small wavelength Görtler vortices in growing boundary layers. The nonlinear states considered in that paper have the 'mean' state driven by the vortices which are themselves trapped between viscous shear layers in which the vortex amplitude decays to zero as a solution of a nonlinear Airy equation. We shall apply this theory to channel flows but with the complication that the mean state is simultaneously driven by the vortices and the TS waves. The 'core equation' to determine the mean state has a significantly different structure in the presence of a TS wave. An important consequence of this change in structure is that vortex states cannot exist beyond a critical TS wave amplitude. Before discussing our problem in more detail, we shall give a brief review of related work on TS-Görtler vortex interactions.

Most of the previous work in this area has in fact been in the context of fully-developed flow. However, one of the earliest papers, Nayfeh (**3**), did consider the external flow case but there the amplitude of a linear Görtler vortex was simply imposed and the linear instability of the resulting flow to an infinitesimal TS wave was considered. The linear Görtler vortex was obtained by ignoring boundary layer growth; since the vortex wavelength cho-

sen was comparable with the boundary layer growth rate we know from the work of Hall (4) that the eigenfunction used by Nayfeh does not satisfy the linear stability equations. Furthermore, the amplitude of a Görtler vortex must be calculated from the Navier-Stokes equations using the approach of Hall (5), Hall (6) or Hall & Lakin (2). Having made the simplification discussed above, Nayfeh found that small vortices have a large effect on TS growth rates. Later Malik (7) repeated Nayfeh's calculations and showed that Nayfeh's conclusions were incorrect and indicated a numerical error in Nayfeh's work.

Subsequently, Bennett & Hall (8) investigated the linear instability of nonlinear vortex flows in curved channels to both 2D and 3D TS waves. Here the nonlinear states were found by solving the full Navier-Stokes equations numerically. The particular TS waves imposed on this flow correspond to the lower branch of the neutral curve. This type of TS wave is particularly relevant in external flows, Smith (9,10), so it is of course important to understand how vortex flows influence this mode even though more unstable modes at finite Reynolds numbers can occur in channel flows. Bennett & Hall (8) showed that vortex flows with wavelengths comparable with the channel width can have a significant destabilizing effect on lower branch TS waves. In a subsequent paper Bennett, Hall & Smith (11) extended the work of (8) to the nonlinear stage where the TS wave has an O(1) effect back on the vortex flow. The vortex wavelengths are then comparable with the channel width and the flow can only be determined by numerical calculations. The somewhat limited number of calculations performed in (11) showed that nonlinear effects prevent the exponential growth of the TS amplitude and that a supercritical bifurcation to a mixed TS-vortex state occurs.

If the vortex wavelength is taken to be long (in fact comparable with the wavelength of the TS wave), a different type of interaction takes place. In this case, Hall & Smith (12) show that initially the interaction is governed by amplitude equations appropriate to a resonant triad. The equations were found to possess a finite time singularity whose structure indicated a more nonlinear state. The latter state is governed by a linear partial differential equation for the vortex coupled to an integro-differential amplitude equation for the TS wave. It was again found, even in the more nonlinear state, that a finite time singularity exists. In a related paper for channel flows, Hall & Smith (13) showed that the vortex velocity field develops a shorter spanwise scale where certain types of singularity occur. Thus, it is important to understand the vortex-TS interaction at smaller wavelengths comparable to or smaller than the channel width since there is some evidence from the work of Hall & Smith (13) and some related boundary layer calculations of Hall & Smith (14) that these shorter scales are induced by an interaction involving longer wavelength vortices.

Finally, in our discussion of previous work we mention the calculation of Daudpota, Hall & Zang (**15**). This interaction problem concerns small amplitude TS waves and vortex states at finite Reynolds numbers at a value of the curvature at which both modes are equally likely. The results of that paper suggest that Görtler vortices can have a significant effect on the equilibration of TS waves.

In the present paper, we consider the interaction of small wavelength Görtler vortices and lower branch TS waves. Our reason for concentrating on these limits is easily explained by reference to the corresponding external flow case. There it is well known that Görtler vortices set up in an experiment conserve their wavelength as they move downstream. Since the boundary layer itself thickens it follows that the local nondimensional vortex wavenumber becomes large as the vortex develops downstream. Thus, the small wavelength limit in the external Görtler problem is appropriate to the ultimate development of any initial fixed wavelength vortex. Similarly, we concentrate on lower branch TS waves since they are the most unstable modes which can be described by formal asymptotic methods.

Since there has been no previous work on small wavelength large amplitude vortices in channel flows, we extend the work of Hall & Lakin (**2**) to fully developed flows. We use the condition of constant mass flow rather than constant pressure gradient and obtain curves of mass flow against pressure gradient in the presence of vortices for different values of the curvature. We show that when vortices develop they cause unusually large increases in the pressure gradient to be induced in order to produce a small increase in the flow rate.

We then consider the effect of a small amplitude TS wave on the above flow structure. Initially the vortex wavelength is taken to be comparable with the channel width so that the interaction equations of Bennett *et al.* (**11**) apply. By taking the further limit of small vortex wavelength, we derive an asymptotic description of a fully nonlinear flow with 'mean' part simultaneously driven by TS waves and Görtler vortices.

We show that vortices can only exist in a finite region bounded by thin shear layers whose structure depends on the size of the TS wave amplitude. We will see that supercritical states exist in the presence of TS waves and that, at a given Taylor number, several equilibrium states with different TS amplitudes and frequencies are possible. We shall show that there is an upper bound for the TS wave size at a given Taylor number. The procedure adopted in the rest of this paper is as follows: in §2 we formulate the nonlinear equations governing 3D flows in curved channels. In §3 we solve these equations for strongly nonlinear vortex flows and in §4 we extend this to allow for the simultaneous presence of TS waves. Finally, in §5 we discuss the results of §3, 4 and draw some conclusions.

§2. Formulation of the problem.

Consider the flow of a fluid of density ρ and kinematic viscosity ν in a curved channel with walls defined by $r' = R_1$ and $r' = R_2 \quad (> R_1)$ with respect to the usual cylindrical polar co-ordinates (r', θ', z'). We assume that the curvature of the channel $\delta = (R_2 - R_1)/R_1$ is small. The basic steady flow considered is that of an azimuthal velocity field driven by an appropriate pressure gradient. It is convenient to define variables x, y, z, t by

$$x = \frac{R_1\theta'}{R_2 - R_1}, \quad y = \frac{r' - R_1}{R_2 - R_1}, \quad z = \frac{z'}{R_2 - R_1}, \quad t = \frac{U_0 t'}{Re(R_2 - R_1)}, \tag{2.1}$$

where U_0 is a typical azimuthal velocity, t is a dimensionless time and $Re \equiv U_0 d/\nu$ is the Reynolds number. Writing the velocity field scaled on U_0 with respect to (x, y, z) as (u, v, w), scaling the pressure on ρU_0^2 , and substituting into the continuity and Navier-Stokes equations yields the system

$$\frac{1}{F}\frac{\partial u}{\partial x} + \frac{\delta u}{F} + \frac{\partial v}{\partial y} + \frac{\partial w}{\partial z} = 0, \tag{2.2a}$$

$$\frac{1}{Re}\left[\nabla^2 - \frac{\partial}{\partial t} - \frac{\delta^2}{F^2}\right]u + \frac{2\delta}{ReF^2}\frac{\partial v}{\partial x} - \frac{1}{F}\frac{\partial p}{\partial x} = Nu + \frac{\delta uv}{F}, \tag{2.2b}$$

$$\frac{1}{Re}\left[\nabla^2 - \frac{\partial}{\partial t} - \frac{\delta^2}{F^2}\right]v - \frac{2\delta}{ReF^2}\frac{\partial u}{\partial x} - \frac{\partial p}{\partial y} = Nv - \frac{\delta u^2}{F}, \tag{2.2c}$$

$$\frac{1}{Re}\left[\nabla^2 - \frac{\partial}{\partial t}\right]w - \frac{\partial p}{\partial z} = Nw, \tag{2.2d}$$

where

$$F = 1 + \delta y, \tag{2.3a}$$

and the operators ∇^2 and N are given by

$$\nabla^2 \equiv \frac{1}{F^2}\frac{\partial^2}{\partial x^2} + \frac{\partial^2}{\partial y^2} + \frac{\partial^2}{\partial z^2} + \frac{\delta}{F}\frac{\partial}{\partial y}, \tag{2.3b}$$

$$N \equiv \frac{u}{F}\frac{\partial}{\partial x} + v\frac{\partial}{\partial y} + w\frac{\partial}{\partial z}. \tag{2.3c}$$

The Taylor number T is given by $T = 2Re^2\delta$, and here we take this to be an O(1) parameter. Dean (**16**) demonstrated that instability of the basic flow given by

$$p = -\frac{Dx}{Re} + O(\delta), \qquad u = \frac{D}{2}(y - y^2) + O(\delta), \tag{2.4}$$

(where D is a constant) occurs first for O(1) axial wavelengths and at an O(1) Taylor number so that here the Reynolds number is large.

We now consider the case of fully nonlinear small wavelength Görtler vortices in the channel and suppose that the mean flow correction to the basic flow in the presence of the vortices is as large as the basic flow itself.

§3. The case of a fully nonlinear Görtler vortex in the channel.

Here we follow the ideas of Hall & Lakin (**2**) who studied the problem of fully nonlinear vortices in an external growing boundary layer. The necessary scalings for the present problem follow those given in that paper with a related flow structure. This structure consists of a vortex activity region (I) defined by $(0 <) y_1 < y < y_2 (< 1)$ say, with thin layers (IIa, b) surrounding $y = y_1$ and $y = y_2$ which act to smooth out the algebraically decaying vortices in the central region. The structure is completed by regions ($IIIa, b$) defined by $0 < y < y_1$ and $y_2 < y < 1$ in which, to leading order, the flow is merely driven by a constant pressure gradient with no vortex present.

Unlike Hall & Lakin (**2**), here our flow velocities (u, v, w) are independent of x and so we seek steady solutions which assume the forms

$$(u, v, w) = \left(U(y,z), \frac{1}{Re}V(y,z), \frac{1}{Re}W(y,z)\right), \quad p = -\frac{Dx}{Re} + \frac{P(y,z)}{Re^2}, \tag{3.1}$$

in the notation of (2.2). Substituting (3.1) into the system (2.2) and ignoring small terms yields, at leading orders, the governing equations

$$\frac{\partial V}{\partial y} + \frac{\partial W}{\partial z} = 0, \tag{3.2a}$$

$$V\frac{\partial U}{\partial y} + W\frac{\partial U}{\partial z} = D + \frac{\partial^2 U}{\partial y^2} + \frac{\partial^2 U}{\partial z^2}, \tag{3.2b}$$

$$V\frac{\partial V}{\partial y} + W\frac{\partial V}{\partial z} + \frac{TU^2}{2} = -\frac{\partial P}{\partial y} + \frac{\partial^2 V}{\partial y^2} + \frac{\partial^2 V}{\partial z^2}, \tag{3.2c}$$

$$V\frac{\partial W}{\partial y} + W\frac{\partial W}{\partial z} = -\frac{\partial P}{\partial z} + \frac{\partial^2 W}{\partial y^2} + \frac{\partial^2 W}{\partial z^2}. \tag{3.2d}$$

We look for a vortex with small axial wavelength $\beta \ll 1$, and use the results of (**2**) that the Taylor number T expands in the manner

$$T = T_0\beta^{-4} + T_1\beta^{-3} + \cdots, \tag{3.3}$$

and that in the main vortex activity region (I) the appropriate velocity and pressure expansions take the forms

$$U = \bar{u}_0 + \beta\bar{u}_1 + \ldots + \{\beta E(U_0^1 + \beta U_1^1 + \ldots) + \beta^2 E^2(U_0^2 + \ldots) + \ldots + c.c\}, \tag{3.4a}$$

$$V = \{\beta^{-1}E(V_0^1 + \beta V_1^1 + \ldots) + E^2(V_0^2 + \ldots) + \ldots + c.c\}, \tag{3.4b}$$

$$W = \{E(W_0^1 + \beta W_1^1 + \ldots) + \beta E^2(W_0^2 + \ldots) + \ldots + c.c\}, \tag{3.4c}$$

$$P = \beta^{-4}\bar{p}_0 + \beta^{-3}\bar{p}_1 + \ldots + \{\beta^{-1}E(P_0^1 + \beta P_1^1 + \ldots) + E^2(P_0^2 + \ldots) + \ldots + c.c\}, \tag{3.4d}$$

where $E \equiv \exp(iz/\beta)$ and $c.c$ denotes the complex conjugate. Notice that in the absence of the vortex the flow reduces to the steady state with $V = W = P = 0$ and $U = \frac{D}{2}(y - y^2)$.

The expansions (3.4) are substituted into (3.2) and powers of β are equated for each Fourier coefficient. The zeroth order equations for the vortex in the core are

$$\frac{dV_0^1}{dy} + iW_0^1 = 0, \qquad U_0^1 + V_0^1\frac{d\bar{u}_0}{dy} = 0, \tag{3.5a, b}$$

$$V_0^1 + T_0U_0^1\bar{u}_0 = 0, \qquad iP_0^1 + W_0^1 = 0, \tag{3.5c, d}$$

and consistency of $(3.5b, c)$ flow in the core

$$T_0\bar{u}_0\frac{d\bar{u}_0}{dy} = 1. \tag{3.6a}$$

Further, the vortex amplitude $|V_0^1|$ follows from the x- momentum equation $(3.2b)$ and satisfies

$$\frac{d^2\bar{u}_0}{dy^2} = -D - 2\frac{d}{dy}\left[\frac{d\bar{u}_0}{dy}|V_0^1|^2\right]. \tag{3.6b}$$

Consequently, the equation $(3.6a)$ for the mean flow fixes the vortex. Integrating $(3.6a)$ gives

$$\bar{u}_0 = \sqrt{\frac{(a + 2y)}{T_0}}, \tag{3.6c}$$

where a is a constant and then $(3.6b)$ yields the condition

$$\frac{d\bar{u}_0}{dy} = b - Dy - 2\frac{d\bar{u}_0}{dy}|V_0^1|^2, \tag{3.6d}$$

where b is another constant. As $|V_0^1|^2$ is non-negative, the extent of the vortex activity region is defined by $|V_0^1| = 0$. If $y = y_1$ and $y = y_2(> y_1)$ are these edges of activity then

$$b = Dy_j + \frac{1}{\sqrt{T_0(a + 2y_j)}}, \tag{3.7}$$

for $j = 1, 2$. The thicknesses of the thin shear layers centered on y_1 and y_2 are found by balancing diffusion across the layers with convection in the streamwise direction and are found to be $O(\beta^{\frac{2}{3}})$. Hence, in the upper layer, we define the $O(1)$ co-ordinate ξ by

$$\xi = \frac{y - y_2}{\beta^{\frac{2}{3}}}. \tag{3.8}$$

The expansions in this region (IIb) are then

$$U = \bar{\bar{u}}_0 + \beta^{\frac{2}{3}}\bar{\bar{u}}_1 + \beta\bar{\bar{u}}_2 + \beta^{\frac{4}{3}}\bar{\bar{u}}_3 + \ldots + \{\beta^{\frac{4}{3}}E(U_{01} + \beta^{\frac{2}{3}}U_{11} + \ldots) + \beta^{\frac{8}{3}}E^2(U_{02} + \ldots) + \ldots + c.c\}, \tag{3.9a}$$

$$V = \{\beta^{-\frac{2}{3}}E(V_{01} + \beta^{\frac{2}{3}}V_{11} + \ldots) + \beta^{\frac{2}{3}}E^2(V_{02} + \ldots) + \ldots + c.c\}, \tag{3.9b}$$

$$W = \{\beta^{-\frac{1}{3}}E(W_{01} + \beta^{\frac{2}{3}}W_{11} + \ldots) + \beta E^2(W_{02} + \ldots) + \ldots + c.c\}, \tag{3.9c}$$

$$P = \beta^{-4}\bar{\bar{p}}_0 + \beta^{-\frac{10}{3}}\bar{\bar{p}}_1 + \ldots + \{\beta^{-\frac{4}{3}}E(P_{01} + \beta^{\frac{2}{3}}P_{11} + \ldots) + \beta^{\frac{2}{3}}E^2(P_{02} + \ldots) + \ldots + c.c\}. \tag{3.9d}$$

The governing equations are very similar to those presented in (**2**) and so we will merely summarize the important features of their solutions. The leading order terms in the mean flow expansion satisfy

$$\frac{d^2\bar{\bar{u}}_0}{d\xi^2} = \frac{d^2\bar{\bar{u}}_1}{d\xi^2} = 0,$$

and matching with the vortex activity region yields

$$\bar{\bar{u}}_0 = \sqrt{\frac{(a+2y_2)}{T_0}}, \qquad \bar{\bar{u}}_1 = \frac{\xi}{\sqrt{T_0(a+2y_2)}}.$$

The governing equations for (U_{01}, V_{01}) are found to be always consistent, but those for U_{11} and V_{11} admit a solution only if a certain solvability requirement is met. This condition is obtained on consideration of higher order mean flow terms and leads to a problem (which is a particular form of the second Painlevé transcendent) given by

$$\frac{d^2V_{01}}{d\xi^2} + \xi\left[\frac{1}{3(a+2y_2)} - \frac{D}{3}\sqrt{T_0(a+2y_2)}\right]V_{01} = \frac{2}{3}V_{01}|V_{01}|^2 - \frac{\sqrt{T_0(a+2y_2)}}{3}fV_{01},$$

where f is some constant whose actual value is not required here. This equation has been shown (**17**) to have a solution for which

$$|V_{01}|^2 \longrightarrow \frac{|\xi|}{2}\left[D\sqrt{T_0(a+2y_2)} - \frac{1}{(a+2y_2)}\right] \qquad \text{as} \quad \xi \longrightarrow -\infty,$$

$$|V_{01}|^2 \longrightarrow 0 \qquad \text{as} \quad \xi \longrightarrow \infty.$$

Thus the fundamental terms U_{01} and V_{01} decay exponentially to zero as $\xi \longrightarrow \infty$ and so the vortex is constrained to lie below y_2. A completely similar analysis holds for the lower shear layer (IIa) at $y = y_1$. We see that the mean flow terms play an essentially passive role in these shear regions, in as much as that the leading order mean flow term and its derivative must be continuous across the shear layers. Outside the vortex activity zone in regions $(IIIa, b)$ we have

$$U = \bar{\bar{u}} + O(\beta^{\frac{2}{3}}),$$

and (3.6b) simplifies to the governing equation $\frac{d^2\bar{u}}{dy^2} = -D$.

Summarizing at this point then, we now have (given T_0) sufficient information so as to enable us to determine the shear layer positions y_1 and y_2 and the constants a, b in (3.6c, d). The leading order mean flow quantity $\bar{u}$ is governed by the following constraints and conditions:

Zone (I).

$$\bar{u} = \sqrt{\frac{(a+2y)}{T_0}}. \tag{3.10a}$$

Zones ($IIIa, b$).

Here

$$\frac{d^2\bar{u}}{dy^2} = -D, \tag{3.10b}$$

and $\bar{u}$ and $\frac{d\bar{u}}{dy}$ are continuous across the shear layers (IIa, b) at y_1 and y_2. From (3.7) we also have

$$Dy_1 + \frac{1}{\sqrt{T_0(a+2y_1)}} = Dy_2 + \frac{1}{\sqrt{T_0(a+2y_2)}}, \tag{3.11}$$

and no-slip conditions $\bar{u} = 0$ on $y = 0, 1$ are imposed.

The constant D is not determined as yet and we choose it so that the non-dimensional mass flux across the channel is kept constant for varying values of T_0. We take the normalization such that $\bar{u} = y - y^2$ in the absence of any vortices so that D is fixed so

$$\int_0^1 \bar{u} dy = \frac{1}{6}. \tag{3.12}$$

We used a simple iterative technique to solve the problem (3.10), (3.11) and it was found that the method was most easily formulated in terms of the quantity T_0D^2. Given this value, a guess was made for the shear of the mean flow at the lower wall $y = 0$ and (3.10b) was integrated to the position y_1 where $T_0\bar{u}\frac{d\bar{u}}{dy} = 1$. Continuity of the mean flow across the shear region (IIa) yielded a value of a on using (3.10a), y_2 was then determined from (3.11) and finally (3.10b) integrated to $y = 1$. If $\bar{u}(1)$ did not vanish, the assumed shear at the lower wall was adjusted until this condition was met. Finally, D was fixed so as to satisfy (3.12).

The results of these calculations are shown in figures (1) & (2). The work of Hall (5) demonstrated that on the basis of linear theory a vortex can exist for $T_0 = T_c = 6\sqrt{3}$. Not surprisingly, our computations revealed that a solution of the problem (3.10)-(3.12) is only possible for $T_0 > T_c$. Also, no solutions occur for $T_0 > 32$ and, indeed, as $T_0 \longrightarrow 32$, the mass constraint (3.12) implies that the pressure gradient $D \longrightarrow \infty$. Figure (1) shows the positions of the shear layers y_1, y_2 as a function of T_0 and as $T_0 \longrightarrow 32$ these positions migrate to the edges of the channel, whereas as T_0 tends to the linear value T_c they merge

at $y = \frac{1}{2}(1 - \frac{1}{\sqrt{3}})$. Figure (2) illustrates the dependence of the Taylor number T_0 on the pressure gradient D.

The normalization we have used to determine D in our calculations thus far is that to ensure a constant non-dimensional mass flow rate. In a realistic experiment, it would be of more interest to determine the dimensional mass flow rate as a function of the total pressure drop along the channel. On recalling the non-dimensionalizations introduced previously, we may easily translate our results so that they may be interpreted in dimensional terms. Figure (3) illustrates the dependence of the dimensional mass flow rate on the pressure drop along the channel. In the absence of any vortices, we know that the mass flux is proportional to the pressure drop, and it is seen that as vortices develop, a large increase in pressure drop is required to produce a small increase in the flow rate. The precise broken curve on figure (3) which is actually followed in any particular experiment is determined by the physical parameters of that experiment, and we see that in each particular case there is a maximum flow rate that can be achieved in the presence of the vortices, irrespective of the size of the pressure gradient.

Lastly in this section, we see that two asymptotic regimes naturally arise here. Firstly, for $T_0 D^2 = 24\sqrt{3} + \delta_*$, $0 < \delta_* \ll 1$, i.e. returning to the case of very small vortices, we find that

$$y_{1,2} = \frac{1}{2}\left(1 - \frac{1}{\sqrt{3}}\right) \mp 3^{-\frac{7}{4}}\delta_*^{\frac{1}{2}} + \ldots,$$

$$a = \left(\frac{\sqrt{3}}{2} - 1\right) + \frac{\delta_*}{9} + \ldots,$$

and $T_0 = 6\sqrt{3} + (\delta_*/2) + \ldots$. These results imply the scalings required for a weakly nonlinear analysis of the vortices along the lines of Hall (**18**).

Secondly, for $\phi \equiv T_0 D^2 \gg 1$, we obtain

$$y_1 = \frac{1}{\phi} + \frac{2^{\frac{7}{4}}}{\phi^{\frac{5}{4}}} + \ldots,$$

$$y_2 = 1 - \left(\frac{8}{\phi}\right)^{\frac{1}{4}} - \frac{1}{16}\left(\frac{8}{\phi}\right)^{\frac{3}{4}} + \ldots,$$

$$a = -\frac{1}{\phi} - \frac{2^{\frac{7}{4}}}{\phi^{\frac{5}{4}}} + \ldots,$$

$$T_0 = 32 - 2^{\frac{23}{4}}\phi^{-\frac{1}{4}} + 2^{\frac{9}{2}}\phi^{-\frac{1}{2}} + \ldots\ .$$

This demonstrates that $T_0 < 32$ in all cases, a restriction which is a direct consequence of the constant non-dimensional mass flow constraint. As T_0 approaches this upper bound the vortices occupy nearly all of the channel and the mean flow profile takes a square root

form everywhere except for thin regions at the sides of the channel. If the non-dimensional flow constraint is relaxed and replaced by a constant pressure gradient requirement, the vortex may then persist for arbitrarily large values of T_0.

The effect on the vortices of introducing TS waves into the channel is now investigated and the scalings are chosen so as to ensure a strong interaction between the vortices and the waves.

§4. Strong interactions between small wavelength Görtler vortices and lower branch TS waves.

We now extend the analysis presented in the last section to the case when TS waves of azimuthal wavenumber $O(Re^{-\frac{1}{7}})$ are also present in the flow. The size of the TS wave is chosen to be such that the nonlinear terms in (2.2) arising from interactions of the TS wave with itself, are of comparable size with the leading order vortex terms. These interactions are most important in the core of the flow away from the viscous wall layers in which the TS wave adjusts to the no slip conditions required at the walls.

Bennett *et al.* (**11**) examined the problem under consideration here but took the vortex and TS wave to vary on an O(1) scale in the z-direction, whereas we choose to study the case of a small axial lengthscale. The TS wave is assumed to be proportional to

$$E \equiv \exp\left[i\left(\alpha x\epsilon - \int^t \frac{\Omega(t)}{\epsilon^4}dt\right)\right], \tag{4.1}$$

where the wavenumber α and the slowly varying frequency Ω are real, and where, anticipating the ensuing analysis, it is found convenient to define the small parameter $\epsilon = Re^{-\frac{1}{7}}$. Away from the viscous wall layers at $y = 0$ and $y = 1$ we follow (**11**) and consider velocity and pressure fields which take the forms

$$u = u_0 + \left(\epsilon^6 u_1 E + c.c\right)\left(1 + O(\epsilon^7)\right), \tag{4.2a}$$

$$v = \frac{\epsilon^7 v_0}{2} + \left(\epsilon^7 v_1 E + c.c\right)\left(1 + O(\epsilon^7)\right), \tag{4.2b}$$

$$w = \frac{\epsilon^7 w_0}{2} + \left(\epsilon^7 w_1 E + c.c\right)\left(1 + O(\epsilon^7)\right), \tag{4.2c}$$

$$p = -Dx\epsilon^7 + \frac{\epsilon^{14} p_0}{2} + \left(\epsilon^8 p_1 E + c.c\right)\left(1 + O(\epsilon^7)\right), \tag{4.2d}$$

where the unknown quantities are independent of x.

Substitution of these forms into the governing equations (2.2) yield that at leading orders the vortex and TS parts of (4.2) satisfy

$$\frac{\partial v_0}{\partial y} + \frac{\partial w_0}{\partial z} = 0, \tag{4.3a}$$

$$\left(\frac{\partial^2}{\partial y^2}+\frac{\partial^2}{\partial z^2}-\frac{\partial}{\partial t}\right)u_0+D=\frac{1}{2}\left(v_0\frac{\partial u_0}{\partial y}+w_0\frac{\partial u_0}{\partial z}\right), \tag{4.3b}$$

$$\left(\frac{\partial^2}{\partial y^2}+\frac{\partial^2}{\partial z^2}-\frac{\partial}{\partial t}\right)v_0-\frac{T}{2}u_0^2-\frac{\partial p_0}{\partial y}=\frac{1}{2}\left(v_0\frac{\partial v_0}{\partial y}+w_0\frac{\partial v_0}{\partial z}\right)$$
$$+2\left[\left(-i\alpha u_1 v_1^*+v_1\frac{\partial v_1^*}{\partial y}+w_1\frac{\partial v_1^*}{\partial z}\right)+c.c\right], \tag{4.3c}$$

$$\left(\frac{\partial^2}{\partial y^2}+\frac{\partial^2}{\partial z^2}-\frac{\partial}{\partial t}\right)w_0-\frac{\partial p_0}{\partial z}=\frac{1}{2}\left(v_0\frac{\partial w_0}{\partial y}+w_0\frac{\partial w_0}{\partial z}\right)$$
$$+2\left[\left(-i\alpha u_1 w_1^*+v_1\frac{\partial w_1^*}{\partial y}+w_1\frac{\partial w_1^*}{\partial z}\right)+c.c\right], \tag{4.3d}$$

and

$$i\alpha u_1+\frac{\partial v_1}{\partial y}+\frac{\partial w_1}{\partial z}=0, \tag{4.4a}$$

$$i\alpha u_0 u_1+\frac{\partial u_0}{\partial y}v_1+\frac{\partial u_0}{\partial z}w_1=0, \tag{4.4b}$$

$$i\alpha u_0 v_1=-\frac{\partial p_1}{\partial y}, \tag{4.4c}$$

$$i\alpha u_0 w_1=-\frac{\partial p_1}{\partial z}. \tag{4.4d}$$

Here the superscript $*$ on a quantity denotes the complex conjugate.

We note that the TS interaction appears at leading order in (4.3c,d). Bennett *et al.*, (**11**), examined the problem with O(1) z-variations but we analyse the limit $\frac{\partial}{\partial z}\longrightarrow\infty$ to obtain an asymptotic description of the long wave-short wave vortex-TS interaction.

If $\beta\ll 1$, but of sufficient size that subsequent expansions in ascending powers of β do not disrupt the leading order equations (4.3, 4.4) we find that on a z-lengthscale of O(β) the leading order vortex and TS quantities assume the forms

$$u_0=\bar{\bar{u}}_0+\ldots+\left\{\beta\left(U_0^1+\ldots\right)\cos\left(\frac{z}{\beta}\right)\right\}+\left\{\beta^2\left(U_1^1+\ldots\right)\cos\left(\frac{2z}{\beta}\right)+\ldots\right\}, \tag{4.5a}$$

$$v_0=\left\{\beta^{-1}\left(V_0^1+\ldots\right)\cos\left(\frac{z}{\beta}\right)\right\}+\left\{\left(V_1^1+\ldots\right)\cos\left(\frac{2z}{\beta}\right)+\ldots\right\}, \tag{4.5b}$$

$$w_0=\left\{\left(W_0^1+\ldots\right)\sin\left(\frac{z}{\beta}\right)\right\}+\left\{\beta\left(W_1^1+\ldots\right)\sin\left(\frac{2z}{\beta}\right)+\ldots\right\}, \tag{4.5c}$$

$$p_0=\beta^{-4}\bar{\bar{p}}_0+\ldots+\left\{\beta^{-1}\left(P_0^1+\ldots\right)\cos\left(\frac{z}{\beta}\right)\right\}+\left\{\beta^2\left(P_1^1+\ldots\right)\cos\left(\frac{2z}{\beta}\right)+\ldots\right\}, \tag{4.5d}$$

and

$$u_1 = \beta^{-2}U_0^\dagger + \ldots + \left\{\beta^{-1}U_1^\dagger \cos\left(\frac{z}{\beta}\right) + \ldots\right\}, \tag{4.6a}$$

$$v_1 = \beta^{-2}V_0^\dagger + \ldots + \left\{\beta^{-1}V_1^\dagger \cos\left(\frac{z}{\beta}\right) + \ldots\right\}, \tag{4.6b}$$

$$w_1 = \beta W_0^\dagger + \ldots + \left\{W_1^\dagger \sin\left(\frac{z}{\beta}\right) + \ldots\right\}, \tag{4.6c}$$

$$p_1 = \beta^{-2}P_0^\dagger + \ldots + \left\{\beta P_1^\dagger \cos\left(\frac{z}{\beta}\right) + \ldots\right\}, \tag{4.6d}$$

where all the unknowns are function of y.

We substitute these expansions into (4.3) & (4.4), together with the relevant expansion $T = T_0\beta^{-4} + \ldots$ for the Taylor number. On equating powers of β associated with each Fourier coefficent we get the solution set

$$U_0^\dagger = A\frac{d\bar{\bar{u}}_0}{dy}, \qquad V_0^\dagger = -i\alpha A\bar{\bar{u}}_0, \qquad P_0^\dagger = \hat{p} - \alpha^2 A\int_0^y(\bar{\bar{u}}_0)^2 dy, \tag{4.7}$$

where the displacement A and pressure term $\hat{p}$ are to be found. Further, we find that

$$U_1^\dagger = A\left(\frac{dU_0^1}{dy} - \frac{2U_0^1}{\bar{\bar{u}}_0}\frac{d\bar{\bar{u}}_0}{dy}\right), \qquad V_1^\dagger = i\alpha AU_0^1, \qquad W_1^\dagger = 2i\alpha A\left(\frac{U_0^1}{\bar{\bar{u}}_0}\frac{d\bar{\bar{u}}_0}{dy} - \frac{dU_0^1}{dy}\right). \tag{4.8}$$

Additionally, the vortex terms U_0^1, V_0^1, W_0^1 satisfy

$$\frac{dV_0^1}{dy} + W_0^1 = 0, \tag{4.9a}$$

$$U_0^1 + \frac{1}{2}\frac{d\bar{\bar{u}}_0}{dy}V_0^1 = 0, \tag{4.9b}$$

$$V_0^1 + \left(2T_0\bar{\bar{u}}_0 - 16\alpha^2|A|^2\frac{d\bar{\bar{u}}_0}{dy}\right)U_0^1 = 0, \tag{4.9c}$$

and the mean flow term $\bar{\bar{u}}_0$ satisfies

$$\frac{d^2\bar{\bar{u}}_0}{dy^2} + D = -\frac{1}{8}\frac{d}{dy}\left(\frac{d\bar{\bar{u}}_0}{dy}(V_0^1)^2\right). \tag{4.9d}$$

Now $(4.9b, c)$ are consistent only if

$$\left(T_0\bar{\bar{u}}_0 - \lambda\frac{d\bar{\bar{u}}_0}{dy}\right)\frac{d\bar{\bar{u}}_0}{dy} = 1, \tag{4.10}$$

where we have put $\lambda \equiv 8\alpha^2|A|^2$.

The TS-vortex interaction requires that the mean flow satisfies (4.10) and then (4.9d) fixes the vortex. The TS wave is governed by the solutions (4.7, 4.8) and is fully determined by considering the wall layers, see below. The consistency condition (4.10) is a generalisation of (3.6a), the additional term stemming from the presence of the TS wave. However, a major difference in the solutions of these two equations exists. Previously, for (3.6a), given $\bar{u}_0$ at some point y^* say, the solution is uniquely defined, whereas now we have

$$\frac{d\bar{\bar{u}}_0}{dy} = \frac{T_0\bar{\bar{u}}_0 \pm \sqrt{(T_0\bar{\bar{u}}_0)^2 - 4\lambda}}{2\lambda}, \tag{4.11}$$

with a consequent ambiguity in the solution. This phenomenon will be found to play a crucial role; for the present we take the negative sign in (4.11) since when $\lambda \longrightarrow 0$ this retrieves the analysis of §3.

We may integrate (4.9d) once to obtain

$$\frac{d\bar{\bar{u}}_0}{dy} + Dy = -\frac{1}{8}\frac{d\bar{\bar{u}}_0}{dy}\left(V_0^1\right)^2 + b,$$

where b is a constant and, as in the previous section, we expect the vortex activity to be concentrated in a region (I) lying between y_1 and y_2 say. The condition that $|V_0^1| \longrightarrow 0$ at these positions together with (4.11) yields the relationship

$$\frac{T_0}{2\lambda}\left[\bar{\bar{u}}_0 - \sqrt{(T_0\bar{\bar{u}}_0)^2 - 4\lambda}\right]_{y=y_1}^{y=y_2} = D(y_1 - y_2). \tag{4.12}$$

We anticipate shear layers at y_1 and y_2 as before, again of thickness $O(\beta^{\frac{2}{3}})$ and which we examine now.

§4.1. The shear layers.

In the shear layer (IIa) centred on y_1, we define the O(1) co-ordinate $\xi = \beta^{-\frac{2}{3}}(y - y_1)$ and the expansions (4.5) & (4.6) are modified to give

$$u_0 = u_0^\dagger + \beta^{\frac{2}{3}}u_1^\dagger + \beta u_2^\dagger + \beta^{\frac{4}{3}}u_3^\dagger + \ldots + \left\{\beta^{\frac{4}{3}}\left(U_{01} + \beta^{\frac{2}{3}}U_{11} + \ldots\right)\cos\left(\frac{z}{\beta}\right)\right\} + \ldots, \tag{4.13a}$$

$$v_0 = \left\{\beta^{-\frac{2}{3}}\left(V_{01} + \beta^{\frac{2}{3}}V_{11} + \ldots\right)\cos\left(\frac{z}{\beta}\right)\right\} + \ldots, \tag{4.13b}$$

$$w_0 = \left\{\beta^{-\frac{1}{3}}\left(W_{01} + \beta^{\frac{2}{3}}W_{11} + \ldots\right)\sin\left(\frac{z}{\beta}\right)\right\} + \ldots, \tag{4.13c}$$

$$p_0 = \beta^{-4}p_0^\dagger + \beta^{-\frac{10}{3}}p_1^\dagger + \ldots + \left\{\beta^{-2}\left(P_{01} + \beta^{\frac{2}{3}}P_{11} + \ldots\right)\cos\left(\frac{z}{\beta}\right)\right\} + \ldots, \tag{4.13d}$$

and

$$u_1 = \beta^{-2}U_{00}^{\dagger} + \beta^{-\frac{4}{3}}U_{01}^{\dagger} + \ldots + \left\{\beta^{-\frac{4}{3}}\left(U_{10}^{\dagger} + \beta^{\frac{2}{3}}U_{11}^{\dagger} + \ldots\right)\cos\left(\frac{z}{\beta}\right)\right\} + \ldots, \qquad (4.14a)$$

$$v_1 = \beta^{-2}V_{00}^{\dagger} + \beta^{-\frac{4}{3}}V_{01}^{\dagger} + \ldots + \left\{\beta^{-\frac{2}{3}}\left(V_{10}^{\dagger} + \beta^{\frac{2}{3}}V_{11}^{\dagger} + \ldots\right)\cos\left(\frac{z}{\beta}\right)\right\} + \ldots, \qquad (4.14b)$$

$$w_1 = \beta W_{00}^{\dagger} + \ldots + \left\{\beta^{-\frac{1}{3}}\left(W_{10}^{\dagger} + \beta^{\frac{2}{3}}W_{11}^{\dagger} + \ldots\right)\sin\left(\frac{z}{\beta}\right)\right\} + \ldots, \qquad (4.14c)$$

$$p_1 = \beta^{-2}P_{00}^{\dagger} + \beta^{-\frac{4}{3}}P_{01}^{\dagger} + \ldots + \left\{\beta^{\frac{2}{3}}\left(P_{10}^{\dagger} + \beta^{\frac{2}{3}}P_{11}^{\dagger} + \ldots\right)\cos\left(\frac{z}{\beta}\right)\right\} + \ldots . \qquad (4.14d)$$

These forms follow from (4.5)–(4.11) and we substitute these expressions into (4.3) & (4.4). As in the previous section, it is found that the mean flow terms $u_0^{\dagger}, u_1^{\dagger}$ satisfy

$$\frac{d^2u_0^{\dagger}}{d\xi^2} = \frac{d^2u_1^{\dagger}}{d\xi^2} = 0.$$

A solvability condition for the fundamental vortex term V_{01} is derived by following the procedure given in §3 and determining circumstances under which the equations governing U_{11} and V_{11} admit a solution. The algebraic manipulation needed now is more complicated than before because of the presence of the TS wave. However, eventually we find that

$$(3 - \lambda\mu_1^2)\mu_1\frac{dV_{01}}{d\xi^2} + \left[T_0\mu_1^3 + D(\lambda\mu_1^2 - 1)\right]\xi V_{01} = \frac{\mu_1}{8}(1 - \lambda\mu_1^2)V_{01}^3 + fV_{01}, \qquad (4.15)$$

where $\mu_1 = \frac{d\bar{u}_0}{dy}\Big|_{y_1}$ and f is some constant. Again, we have an unscaled form of the second Painlevé transcendent, and the solution has the desired property that $V_{01} \longrightarrow 0$ as $\xi \longrightarrow -\infty$ and $V_{01} = O(\xi^{\frac{1}{2}})$ as $\xi \longrightarrow \infty$, as long as

$$S_1 \equiv \frac{T_0\mu_1^3 + D(\lambda\mu_1^2 - 1)}{\mu_1(1 - \lambda\mu_1^2)} > 0. \qquad (4.16a)$$

An entirely analogous analysis is appropriate for the shear layer (IIb) positioned at $y = y_2$ and the resulting Painlevé problem is precisely (4.15) but with μ_1 replaced throughout by $\mu_2 = \frac{d\bar{u}_0}{dy}\Big|_{y_2}$. Again, the fundamental vortex term V_{01} decays exponentially as we move away from region (I) if

$$S_2 \equiv \frac{T_0\mu_2^3 + D(\lambda\mu_2^2 - 1)}{\mu_2(1 - \lambda\mu_2^2)} < 0. \qquad (4.16b)$$

The conditions (4.16) may only be checked by numerical computations and so at this stage we assume that they hold. The fundamental terms $U_{10}^{\dagger}, \ldots, P_{10}^{\dagger}$ associated with the TS wave in expansions (4.14) are expressible in terms of the vortex coefficients $U_{01}, \ldots, P_{01}$.

The exponential decay of these latter terms imply a similar behavior for the former and so outside regions (I) & (IIa,b), the implied velocity and pressure fields develop as

$$u_0 = \hat{\bar{\bar{u}}}_0 + \ldots, \qquad u_1 = \beta^{-2}\hat{U}_0^{\dagger} + \ldots, \tag{4.17a,e}$$

$$v_0 = 0 + \ldots, \qquad v_1 = \beta^{-2}\hat{V}_0^{\dagger} + \ldots, \tag{4.17b,f}$$

$$w_0 = 0 + \ldots, \qquad w_1 = \beta\hat{W}_0^{\dagger} + \ldots, \tag{4.17c,g}$$

$$p_0 = \beta^{-4}\hat{\bar{\bar{p}}}_0 + \ldots, \qquad p_1 = \beta^{-2}\hat{P}_0^{\dagger} + \ldots, \tag{4.17d,h}$$

to leading order. We find that, as in regions $(IIIa,b)$ examined in §3, the mean flow quantity $\hat{\bar{\bar{u}}}_0$ is simply given by

$$\frac{d^2\hat{\bar{\bar{u}}}_0}{dy^2} = -D, \tag{4.18a}$$

and here the TS parts $\hat{U}_0^{\dagger}, \hat{V}_0^{\dagger}$ satisfy

$$\hat{U}_0^{\dagger} = A\frac{d\hat{\bar{\bar{u}}}_0}{dy}, \qquad \hat{V}_0^{\dagger} = -i\alpha A\hat{\bar{\bar{u}}}_0. \tag{4.18b}$$

Finally, to complete the flow structure which thus far has been identical to that given in §3, we add wall layers at $y = 0, 1$. In the layer at $y = 0$, we define the O(1) co-ordinate by $y = \epsilon^2 Y$ and the fluid velocity and pressure expand as

$$u = \epsilon^2\hat{\hat{U}}_{0L} + \ldots + \left(\epsilon^6\beta^{-2}\hat{\hat{U}}_{1L}E + \ldots + c.c.\right)\left(1 + O(\epsilon^7)\right),$$

$$v = \left(\epsilon^9\beta^{-2}\hat{\hat{V}}_{1L}E + \ldots + c.c.\right)\left(1 + O(\epsilon^7)\right),$$

$$w = \left(\epsilon^7\beta\hat{\hat{W}}_{1L}E + \ldots + c.c.\right)\left(1 + O(\epsilon^7)\right),$$

$$p = -Dx\epsilon^7 + \frac{\epsilon^{14}}{2}\left(\beta^{-4}\hat{\hat{P}}_{0L} + \ldots\right) + \left(\epsilon^8\beta^{-2}\hat{\hat{P}}_{1L}E + \ldots + c.c.\right)\left(1 + O(\epsilon^7)\right).$$

Substituting these expressions into the governing equations (2.2) leads to the usual lower branch TS wave eigenproblem, see for example (8). We find that the TS pressure on the lower wall $Y = 0$ is given by

$$\hat{\hat{P}}_{1L} = \frac{A\lambda_L^{\frac{5}{3}}Ai'(\hat{\xi}_L)}{(i\alpha)^{\frac{1}{3}}\left(\int_{\hat{\xi}_L}^{\infty} Ai(\xi)d\xi\right)},$$

where λ_L is the shear of the mean flow $\hat{\bar{\bar{u}}}_0$ at the wall, Ai is the Airy function (see (19)) and $\hat{\xi}_L = -i^{\frac{1}{3}}\Omega/(\alpha\lambda_L)^{\frac{2}{3}}$. Consideration of the upper wall leads to a similar TS pressure at

$y = 1$ and using equation (4.7c) for the leading order TS pressure across the whole of the channel, we finally obtain

$$i^{\frac{1}{3}}\alpha^{\frac{7}{3}}\left(\int_0^1(\bar{\tilde{u}}_0)^2dy\right) = \frac{\lambda_L^{\frac{5}{3}}Ai'(\hat{\xi}_L)}{\left(\int_{\hat{\xi}_L}^{\infty}Ai(\xi)d\xi\right)} + \frac{\lambda_U^{\frac{5}{3}}Ai'(\hat{\xi}_U)}{\left(\int_{\hat{\xi}_U}^{\infty}Ai(\xi)d\xi\right)}, \tag{4.19}$$

as the eigenrelation to determine the neutral wavenumber α and frequency Ω. In this formula, λ_U is the shear of the mean flow at the upper wall and $\hat{\xi}_U = -i^{\frac{1}{3}}\Omega/(\alpha\lambda_U)^{\frac{2}{3}}$.

We now have sufficient knowledge so as to completely specify the problem. In the core region the leading order mean flow satisfies (4.10) and (assuming that (4.16a,b) hold) has continuous first derivative at the shear layers y_1 and y_2. These shear layer positions satisfy (4.12) and outside the core the mean flow is determined by (4.18a). The imposition of zero velocity conditions at the walls now (in principle) yields the complete mean flow across the channel to within an arbitrary constant. This degree of freedom is fixed by choosing the pressure gradient D so as to ensure constant non-dimensional mass flux and, finally, (4.19) yields the wavenumber α and frequency Ω of the TS wave.

Analysis of the governing system reveals that it is convenient to define $\hat{\lambda}$ by $\lambda = \hat{\lambda}T_0$. The problem is then easily formulated in terms of the parameter groupings T_0D^2 and $\hat{\lambda}$. If we write the mean flow in region ($IIIa$), (where (4.18a) holds) as

$$\bar{\tilde{u}}_0 = D\left(\Phi y - \frac{y^2}{2}\right), \tag{4.20a}$$

where Φ is an initial guess for the shear at the lower wall, then the position y_1 of the lower shear layer satisfies

$$\left[\Phi y_1 - \frac{y_1^2}{2} - \hat{\lambda}\left(\Phi - y_1\right)\right]\left(\Phi - y_1\right) = \frac{1}{T_0D^2}. \tag{4.20b}$$

It has already been noted that an ambiguity appears to exist as to which sign to take in the expression (4.11). However, it is easily shown that if the positive sign is taken, then it is not possible for (4.10) to hold for any $y > y_1$; consequently no upper shear layer could exist and the flow structure described would not be valid. We are thus led to the conclusion that the negative sign should be taken in (4.11), and if we write $\bar{\tilde{u}}_0 = D\hat{U}$, the solution of (4.11) is of the form

$$\frac{T_0D^2}{4}\hat{U}^2 + \frac{T_0D^2}{4}\sqrt{\hat{U}^2 - \frac{4\hat{\lambda}}{T_0D^2}} - \hat{\lambda}\ln\left[\sqrt{\frac{T_0D^2}{4\hat{\lambda}}}\left(\hat{U} + \sqrt{\hat{U}^2 - \frac{4\hat{\lambda}}{T_0D^2}}\right)\right] = y + const., \tag{4.20c}$$

where the constant is chosen to ensure continuity in $\bar{\tilde{u}}_0$ across y_1. Equation (4.20c) together with (4.12) which now assumes the form

$$\frac{1}{2\hat{\lambda}}\left[\hat{U} - \sqrt{\hat{U}^2 - \frac{4\hat{\lambda}}{T_0D^2}}\right]_{y=y_1}^{y=y_2} = y_1 - y_2, \tag{4.20d}$$

yields y_2 and the mean flow and its derivative at $y = y_2$. For $y > y_2$, we revert to the equation

$$\frac{d^2\bar{u}_0}{dy^2} = -D,$$

which is integrated to the upper wall, $y = 1$. A simple Newton iteration is applied to the guess for the lower wall shear value Φ to ensure that $\bar{u}_0$ vanishes at $y = 1$. The constant D is then fixed so as to give constant mass flux and (4.19) gives α and Ω.

The computations were initially performed by fixing T_0D^2 and then repeatedly solving the problem for increasing values of $\hat{\lambda}$ from $\hat{\lambda} = 0$. We note that the limit $\hat{\lambda} \longrightarrow 0$ corresponds to the problem considered in §3 where no TS wave is present. As in the work presented there, no solutions were found for $T_0D^2 < 24\sqrt{3}$. For small values of T_0D^2 up to approximately 80, as $\hat{\lambda}$ was increased the shear layer positions y_1 and y_2 monotonically increased and decreased respectively until a critical value of $\hat{\lambda}$ was reached (dependent upon T_0D^2) at which stage y_1 and y_2 merged. At this point, the vortex disappeared and the problem reduced to that of a channel flow with a small TS wave imposed with the resulting neutral wavenumber and frequency $\alpha = 5.7834$, $\Omega = 7.4016$. This critical value of $\hat{\lambda}$, say $\hat{\lambda}_c$ is determined by demanding that equation (4.20*b*) with $\Phi = 1$ has a double root at $y = y_1$. For $\hat{\lambda} > \hat{\lambda}_c$, the only solution which exists is plane Poiseuille flow with no vortex and a linear 2D-TS wave of arbitrary amplitude imposed.

For values of $T_0D^2 >\approx 80$, a different behavior was observed. As $\hat{\lambda}$ was increased, but prior to y_1 and y_2 merging, the solution apparently vanished, although solutions could again be generated in a neighborhood of $\hat{\lambda}_c(T_0D^2)$ defined in the previous paragraph. It was noted that as this breakdown position was approached the value S_1 defined in (4.16*a*) approached zero and, in turn, this ensures that the two possible values of $\left(\frac{d\bar{u}_0}{dy}\right)$ at $y = y_1$, given in (4.11), merge. A detailed description of the results of these and the subsequent numerical solutions will be given in §5 where the significance of the results will also be discussed.

If $\hat{\lambda}_{B1}(T_0D^2)$ and $\hat{\lambda}_{B2}(T_0D^2)$ are respectively the values of $\hat{\lambda}$ at which breakdown occurs as $\hat{\lambda}$ is increased from zero and decreased from $\hat{\lambda}_c$, at these values the Painlevé problem (4.15) at $y = y_1$ clearly becomes inapplicable. The shear layer is again of thickness $O(\beta^{\frac{2}{3}})$ but the fluid quantities now behave as

$$u_0 = u_0^{\dagger} + \beta^{\frac{2}{3}}u_1^{\dagger} + \beta u_2^{\dagger} + \ldots + \left\{\beta^{\frac{7}{6}}\left(U_{01} + \beta^{\frac{1}{3}}U_{11} + \ldots\right)\cos\left(\frac{z}{\beta}\right)\right\} + \ldots, \qquad (4.21a)$$

$$v_0 = \left\{\beta^{-\frac{5}{6}}\left(V_{01} + \beta^{\frac{1}{3}}V_{11} + \ldots\right)\cos\left(\frac{z}{\beta}\right)\right\} + \ldots, \qquad (4.21b)$$

$$w_0 = \left\{\beta^{-\frac{1}{2}}\left(W_{01} + \beta^{\frac{1}{3}}W_{11} + \ldots\right)\sin\left(\frac{z}{\beta}\right)\right\} + \ldots, \qquad (4.21c)$$

$$p_0 = \beta^{-4} p_0^{\dagger} + \beta^{-\frac{10}{3}} p_1^{\dagger} + \ldots + \left\{ \beta^{-\frac{13}{6}} \left(P_{01} + \beta^{\frac{1}{3}} P_{11} + \ldots \right) \cos\left(\frac{z}{\beta} \right) \right\} + \ldots, \qquad (4.21d)$$

and

$$u_1 = \beta^{-2} U_{00}^{\dagger} + \beta^{-\frac{5}{3}} U_{01}^{\dagger} + \ldots + \left\{ \beta^{-\frac{3}{2}} \left(U_{10}^{\dagger} + \beta^{\frac{1}{3}} U_{11}^{\dagger} + \ldots \right) \cos\left(\frac{z}{\beta} \right) \right\} + \ldots, \qquad (4.22a)$$

$$v_1 = \beta^{-2} V_{00}^{\dagger} + \beta^{-\frac{4}{3}} V_{01}^{\dagger} + \ldots + \left\{ \beta^{-\frac{5}{6}} \left(V_{10}^{\dagger} + \beta^{\frac{1}{3}} V_{11}^{\dagger} + \ldots \right) \cos\left(\frac{z}{\beta} \right) \right\} + \ldots, \qquad (4.22b)$$

$$w_1 = \beta W_{00}^{\dagger} + \ldots + \left\{ \beta^{-\frac{1}{2}} \left(W_{10}^{\dagger} + \beta^{\frac{1}{3}} W_{11}^{\dagger} + \ldots \right) \sin\left(\frac{z}{\beta} \right) \right\} + \ldots, \qquad (4.22c)$$

$$p_1 = \beta^{-2} P_{00}^{\dagger} + \beta^{-\frac{4}{3}} P_{01}^{\dagger} + \ldots + \left\{ \beta^{\frac{1}{2}} \left(P_{10}^{\dagger} + \beta^{\frac{1}{3}} P_{11}^{\dagger} + \ldots \right) \cos\left(\frac{z}{\beta} \right) \right\} + \ldots, \qquad (4.22d)$$

where these expansions follow from the solutions in region (I) and the breakdown assumption

$$T_0 \mu_1^3 = D(1 - \lambda \mu_1^2),$$

from $(4.16a)$. We may retrieve a solvability condition for the fundamental vortex term V_{01} which takes the form

$$\frac{d^2 V_{01}}{d\xi^2} + \frac{T_0}{2\lambda} \xi V_{01} = \frac{V_{01}}{128} \left(V_{01}^2 - f_* \right)^2, \qquad (4.23)$$

where f_* is a constant, *c.f.* (4.15). This equation has a solution with $V_{01} = \mathrm{O}(\xi^{\frac{1}{4}})$ as $\xi \longrightarrow \infty$ (which matches with the behavior of the quantity V_0^1 in the core as $y \longrightarrow y_1$) and exponential decay as $\xi \longrightarrow -\infty$, and so the overall flow structure elucidated already remains valid. We note that at $\hat{\lambda} = \hat{\lambda}_{B1}, \hat{\lambda}_{B2}$ the structure of the upper shear layer at y_2 is not affected (i.e. $S_2 < 0$ in $(4.16b)$) and so the modified version of the second Painlevé transcendent is still the governing equation there.

§4.2. A model problem for the case $\hat{\lambda}_{B1} < \hat{\lambda} < \hat{\lambda}_{B2}$.

We conjecture that a new solution structure must govern the flow for the range of $\hat{\lambda}$ between the breakdown points. To examine this case, we considered the simpler model problem given by

$$\epsilon^2 \frac{d^2 U}{dy^2} = U \left[\frac{1}{T_*} + \hat{\lambda}_* \left(\frac{du}{dy} \right)^2 - u \frac{du}{dy} \right], \qquad (4.24a)$$

$$\frac{du}{dy} = A - y - \frac{du}{dy} U^2, \qquad (4.24b)$$

with $0 < \epsilon \ll 1$, $u(0) = u(1) = U(0) = U(1) = 0$ and where A is some constant to be determined. The relevance of this system to the problem at hand is thus; here we expect to have a central region where $U = O(1)$ and

$$\frac{1}{T_*} + \hat{\lambda}_* \left(\frac{du}{dy}\right)^2 - u\frac{du}{dy} = 0, \tag{4.25}$$

(c.f. (4.10)), bounded by thin regions in which U changes rapidly to zero (c.f. shear regions (II)) and in the remainder of the channel $\frac{du}{dy} \approx A - y$, (c.f. regions $(IIIa, b)$). Numerical solution of (4.24) for ϵ small but non-zero revealed the existence of a non-trivial solution for all $0 < \hat{\lambda}_*$ until the critical value of this parameter was reached at which the 'shear layer' positions merged. This further suggests that a new structure for the asymptotic problem comes into play at some stage.

For asymptotically small ϵ, the structure proposed in §§4, 4.1 is valid for this model problem for $0 < \hat{\lambda}_* < \hat{\lambda}^*_{B1}(T_*)$ and $\hat{\lambda}_* > \hat{\lambda}^*_{B2}(T_*)$, say where $\hat{\lambda}^*_{B1}(T_*)$ and $\hat{\lambda}^*_{B2}(T_*)$ are the breakdown points described before. For $\hat{\lambda}^*_{B1}(T_*) < \hat{\lambda}_* < \hat{\lambda}^*_{B2}(T_*)$, we suppose that a shear layer exists at $y = y_1^*$, and that it has thickness $O(\epsilon)$, i.e., much thinner than the previous $O(\epsilon^{\frac{2}{3}})$ size. If in the vicinity of y_1^* we define the O(1) co-ordinate ψ by

$$y - y_1^* = \epsilon\psi, \tag{4.26a}$$

then the functions U, u behave as

$$U = U_0 + \ldots, \qquad u = \phi_0 + \epsilon u_0 + \ldots, \tag{4.26b}$$

locally. Here $\phi_0 \equiv Ay_1^* - (y_1^{*2}/2)$ is the value of u at $y = y_1^*$, and we further suppose that just below y_1^* we have $\frac{du}{dy} = \phi_1 \equiv A - y_1^*$ and $U \longrightarrow 0$. Putting (4.26) into (4.24) yields the system

$$\frac{du_0}{d\psi} = \frac{\phi_1}{1 + U_0^2}, \tag{4.27a}$$

$$\frac{d^2U_0}{d\psi^2} = U_0\left[\frac{1}{T_*} + \hat{\lambda}_*\left(\frac{du_0}{d\psi}\right)^2 - \phi_0\left(\frac{du_0}{d\psi}\right)\right]. \tag{4.27b}$$

Equation (4.27b) may be integrated once to obtain the solution

$$\left(\frac{dU_0}{d\psi}\right)^2 = \left[\frac{U_0^2}{T_*} + \hat{\lambda}_*\phi_1^2\left(\frac{U_0^2}{1 + U_0^2}\right) - \phi_0\phi_1 \ln\left(1 + U_0^2\right)\right],$$

which satisfies $\frac{dU_0}{d\psi}, \frac{d^2U_0}{d\psi^2} \longrightarrow 0$ as $U_0 \longrightarrow 0$.

These equations admit a solution in which $\frac{du_0}{d\psi} \longrightarrow \phi_1^*$ $(< \phi_1)$ as $\psi \longrightarrow \infty$ (and so $U_0 \longrightarrow const.$ from (4.27a)) where

$$\frac{1}{T_*} + \hat{\lambda}_*\phi_1\phi_1^* - \phi_0\phi_1\phi_1^*\left[\frac{\ln\left(\frac{\phi_1}{\phi_1^*}\right)}{(\phi_1 - \phi_1^*)}\right] = 0. \tag{4.28}$$

Further, we fix ϕ_1^* to satisfy (4.25) so that

$$\frac{1}{T_*} + \hat{\lambda}_* (\phi_1^*)^2 - \phi_0 \phi_1^* = 0, \tag{4.29}$$

and across the central region u is governed by the solution of

$$\frac{du}{dy} = \frac{1}{2\hat{\lambda}_*} \left[u - \sqrt{u^2 - \frac{4\hat{\lambda}_*}{T_*}} \right], \tag{4.30}$$

subject to $u(y_1^*) = \phi_0$. Finally, the upper shear layer position y_2^* is determined (using (4.24*b*)) by

$$y_1^* - y_2^* = \frac{1}{2\hat{\lambda}_*} \left[u - \sqrt{u^2 - \frac{4\hat{\lambda}_*}{T_*}} \right] \Bigg|_{y=y_2^*} - \phi_1, \tag{4.31}$$

and for all the problems encountered in this paper, the shear layer at y_2^* was found to be of the thicker $O(\epsilon^{\frac{2}{3}})$ variety with the usual Painlevé-type governing equation.

To summarize this new structure, we have shown that now a thinner shear layer may exist across which u is continuous and $\frac{du}{dy}$ suffers a discontinuity. In this layer, the 'vortex' term U is of size O(1) in contrast to its much smaller magnitude in the case of the $O(\epsilon^{\frac{2}{3}})$ layer structure of §4.1. This term tends to zero as we move away from the core and to an O(1) constant as we approach the core. The calculation for $\hat{\lambda}_{B1}^*(T_*) < \hat{\lambda}_* < \hat{\lambda}_{B2}^*(T_*)$ was tackled in the following manner.

As before, the shear for the 'mean flow' quantity u at the lower wall (A in (4.24*b*)) was guessed. Previously, for the thicker shear layer, the position of the lower layer was determined by demanding that (4.25) be satisfied, but now this is no longer the required condition. Instead, we now solve (4.28) & (4.29) for ϕ_1 and ϕ_1^* and hence determine y_1^*. In turn, (4.30) & (4.31) are used to find y_2^*, above which $U \longrightarrow 0$ exponentially and $u(1)$ found using (4.24). A Newton iteration on A is then used to ensure that $u(1) = 0$. This calculation demonstrated that the solution structure proposed was the required one for $\hat{\lambda}_{B1}^*(T_*) < \hat{\lambda}_* < \hat{\lambda}_{B2}^*(T_*)$, so that depending on the values of $\hat{\lambda}_*$ and T_* one of the two distinct structures provided the solution to our problem.

The result of this investigation of the model problem suggested that a similar phenomenon of a change in the asymptotic solution structure may occur in the vortex-TS interaction problem under consideration. If for $\hat{\lambda}_{B1} < \hat{\lambda} < \hat{\lambda}_{B2}$ we seek a structure with the lower shear layer at y_1 of size $O(\beta)$, then the solutions for the unknowns of (4.5) & (4.6) in the region of vortex activity suggest that in the shear region where now $\xi = (y - y_1)/\beta$, we have

$$u_0 = u_0^\dagger + \beta u_1^\dagger + \ldots + \left\{ \beta \left(U_{01} + \beta U_{11} + \ldots \right) \cos\left(\frac{z}{\beta} \right) \right\} + \ldots, \tag{4.32a}$$

$$v_0 = \left\{\beta^{-1}\left(V_{01} + \beta V_{11} + \ldots\right)\cos\left(\frac{z}{\beta}\right)\right\} + \ldots, \tag{4.32b}$$

$$w_0 = \left\{\beta^{-1}\left(W_{01} + \beta W_{11} + \ldots\right)\sin\left(\frac{z}{\beta}\right)\right\} + \ldots, \tag{4.32c}$$

$$p_0 = \beta^{-4}p_0^{\dagger} + \ldots + \left\{\beta^{-3}\left(P_{01} + \beta P_{11} + \ldots\right)\cos\left(\frac{z}{\beta}\right)\right\} + \ldots, \tag{4.32d}$$

and

$$u_1 = \beta^{-2}U_{00}^{\dagger} + \ldots + \left\{\beta^{-2}\left(U_{10}^{\dagger} + \beta U_{11}^{\dagger} + \ldots\right)\cos\left(\frac{z}{\beta}\right)\right\} + \ldots, \tag{4.33a}$$

$$v_1 = \beta^{-2}V_{00}^{\dagger} + \ldots + \left\{\beta^{-1}\left(V_{10}^{\dagger} + \beta V_{11}^{\dagger} + \ldots\right)\cos\left(\frac{z}{\beta}\right)\right\} + \ldots, \tag{4.33b}$$

$$w_1 = \beta W_{00}^{\dagger} + \ldots + \left\{\beta^{-1}\left(W_{10}^{\dagger} + \beta W_{11}^{\dagger} + \ldots\right)\sin\left(\frac{z}{\beta}\right)\right\} + \ldots, \tag{4.33c}$$

$$p_1 = \beta^{-2}P_{00}^{\dagger} + \ldots + \left\{\left(P_{10}^{\dagger} + \beta P_{11}^{\dagger} + \ldots\right)\cos\left(\frac{z}{\beta}\right)\right\} + \ldots, \tag{4.33d}$$

instead of (4.13) & (4.14). After substituting these expansions into equations (4.3) & (4.4) and some manipulation, we find that $u_0^{\dagger} = const.$ (= ϕ_0 say, in the notation of the model problem discussion) and that we have the solvability problem

$$\frac{d^4V_{01}}{d\xi^4} - 2\frac{d^2V_{01}}{d\xi^2} + V_{01} + T_0\phi_0U_{01} = \lambda(U_{01} + \hat{\hat{V}}_{01}\frac{du_1^{\dagger}}{d\xi}, \tag{4.34a}$$

$$\hat{\hat{V}}_{01} - \frac{d^2\hat{\hat{V}}_{01}}{d\xi^2} = U_{01} + \frac{d^2U_{01}}{d\xi^2}), \tag{4.34b}$$

$$\frac{du_1^{\dagger}}{d\xi} = \phi_1 + \frac{U_{01}V_{01}}{4}, \tag{4.34c}$$

$$\frac{d^2U_{01}}{d\xi^2} - U_{01} = \frac{1}{2}V_{01}\left(\frac{du_1^{\dagger}}{d\xi}\right), \tag{4.34d}$$

where $V_{10}^{\dagger} = i\alpha A\hat{\hat{V}}_{01}$ and ϕ_1 is a constant. To meet the boundary conditions required we need to specify that the vortex decays exponentially below y_1 so that $U_{01}, V_{01}, V_{10}^{\dagger} \longrightarrow 0, \frac{du_1^{\dagger}}{d\xi} \longrightarrow \phi_1$ as $\xi \longrightarrow -\infty$. We additionally need $\frac{du_1^{\dagger}}{d\xi}$ and the vortex terms to approach non-zero constants as $\xi \longrightarrow \infty$. That (4.34) admits such a solution is not immediately obvious, but this system bears close analogy with the model problem already discussed. If the full problem is derived with a small parameter multiplying the pressure in the axial momentum equation then, if this parameter is allowed to tend to zero, we recover the model equation. The structure of (4.34), together with the similarity with the model (4.24) and

the subsequent solution of that system suggest strongly that a solution of (4.34) with the required behavior exists.

If the mean flow quantity $\bar{\bar{u}}_0$ inside the activity region is defined by $\bar{\bar{u}}_0 = DU$ as before, then here

$$\frac{dU}{dy} = \frac{1}{2\hat{\lambda}}\left[U - \sqrt{U^2 - \frac{4\hat{\lambda}}{T_0 D^2}}\right], \qquad U(y_1) = \phi_0, \tag{4.35a}$$

and y_2 is given by

$$y_1 - y_2 = \frac{1}{2\hat{\lambda}}\left[U - \sqrt{U^2 - \frac{4\hat{\lambda}}{T_0 D^2}}\right]\Bigg|_{y=y_2} - \phi_1, \tag{4.35b}$$

where (4.28) & (4.29) are to be satisfied with T_* replaced by $T_0 D^2$ in these equations.

This modified structure was then used to numerically solve the interaction problem for $\hat{\lambda}_{B1} < \hat{\lambda} < \hat{\lambda}_{B2}$. The results and some discussion are now given in §5.

§5. Results and discussion.

We now discuss the results for the strongly nonlinear TS-vortex interaction which can be found using the scheme outlined in the previous section. We note that the numerical scheme used allows for the possibility that the lower shear layer bounding the region of vortex activity to be either of thickness $O(\beta^{\frac{2}{3}})$ or $O(\beta)$ depending on the properties of the core equation (4.10) at y_1.

In figure (4), we have shown the dependence of D on the Taylor number T_0 for several values of $\hat{\lambda} = \lambda/T_0$ which characterizes the size of the TS wave. We note that all the curves terminate on the line $D = 2$ at which point there is no vortex activity and the flow reduces to plane Poiseuille flow with a superimposed two-dimensional TS wave of arbitrary amplitude. The wavenumber α and the frequency Ω of course vary on each of the curves and on $D = 2$ α and Ω have the linear neutral values for plane Poiseuille flow, namely $\alpha = 5.7834$, $\Omega = 7.4016$. In figure (5), we have shown the development of two of these curves at higher values of T_0. The shapes of these curves are typical of the results we found for all $\hat{\lambda}$, thus when $T_0 \longrightarrow \infty$, we have $D \longrightarrow \infty$ but $D/T_0 \longrightarrow 0$.

In figure (6), we show the variations of the shear layer positions y_1 and y_2 with T_0 for the cases of $\hat{\lambda} = 0.01$ and $\hat{\lambda} = 0.2$. The values of y_1 which correspond to the Painlevé transition layer as opposed to the structure discussed in §4.2 are indicated by the part of the curve which lies between the crosses marked on figure (6). The values of y_1 and y_2 coalesce when $D \longrightarrow 2$ in which case the basic state in the absence of the vortices is simply plane Poiseuille flow. The mean velocity profiles corresponding to figures (5*ii*), (6*ii*) are

shown in figure (7) for a few representative values of T_0. For $\hat{\lambda} = 0.2$ vortices may only exist for $T_0 > 19.06$ and the Painlevé shear problem at y_1 switches to the other structure with a much thinner shear layer when $T_0 \approx 21$. In figure (7*i*), for which $T_0 = 19.98$ the mean flow has a continuous derivative at y_1 and the overall profile is not much changed from the plane Poiseuille case $T_0 < 19.06$. In figure (7*ii*), $T_0 = 23.52$ and the discontinuity in the derivative of the mean flow at y_1 is clear now that the very thin shear layer structure has taken over. For even higher Taylor numbers ($T_0 = 26.61$ in fig. (7*iii*)) this discontinuity becomes increasingly more marked.

It should be stressed that figures (5) & (6) do not describe directly the bifurcation structure of a finite amplitude TS wave where T_0 or D varies. In an experimental setting, the TS wave is often generated by a vibrating ribbon so that as it moves downstream its frequency is constant. The bifurcation picture for constant frequency TS waves can be deduced from figure (4) if the lines of constant Ω are plotted. However, it is easier to calculate the bifurcation curves by modifying the algorithm described in §4 to allow for an outer loop in which we can iterate on $T_0 D^2$ to make Ω constant.

In figure (8), we show the bifurcation pictures for five fixed frequency TS waves. We take $\alpha|A|$ as a representative TS amplitude and show how this quantity varies with T_0 for the frequencies chosen. We see that in each case there is a supercritical bifurcation to a finite amplitude mixed vortex-TS state. At the bifurcation point on the horizontal axis the TS wave has zero amplitude and the basic state is the fully nonlinear vortex flow described in section 3.

Solutions for the nonlinear vortex state have been shown to exist only for Taylor numbers $T_0 < 32$. Calculations performed for increasingly large values of Ω (curves for $\Omega = 1200$ & 1600 are shown in figure (8)) suggest that for Taylor numbers $T_0 > 32$ TS waves of arbitrarily small amplitude are possible. As $\Omega \longrightarrow 7.4016$ there is a limiting bifurcation curve (dotted in figure (8) and labelled C_1) corresponding to the linear neutral frequency for TS waves in Poiseuille flow. We note that it is straightforward to show that for large T_0 the amplitude of the TS wave on C_1 is proportional to T_0. All the bifurcation curves lie to the right of C_1 and joins the horizontal axis at a point $6\sqrt{3} < T_0 < 32$.

Now let us turn to the physical implications of the above results. Firstly suppose that the Taylor number is fixed. If T_0 is less than the linear critical value $6\sqrt{3}$, then the only possible state is plane Poiseuille flow. If T_0 lies in the range $6\sqrt{3} < T_0 < 32$, then there exists either a mixed TS-vortex state, a finite amplitude vortex state or plane Poiseuille flow. Since the mixed state bifurcates supercritically from the vortex state, it is presumably the only available stable solution of the vortex-TS interaction equations. In this Taylor number range, there is an upper limit to the size of the TS wave which the vortex flow can

tolerate. Thus, when C_1 is approached the vortices decay and the azimuthal velocity field reduces to plane Poiseuille flow. Where C_1 is crossed the vortex-TS interaction equations no longer determine the size of the TS wave which will then be fixed by a weakly nonlinear theory based on the Stuart-Watson method. Thus, in the Taylor number region where a strongly nonlinear vortex flow exists, the imposition of a TS wave of gradually increasing size ultimately destroys the vortex state and sets up a flow comprising plane Poiseuille flow and a two-dimensional TS wave. At Taylor numbers beyond 32, the range of values of $\alpha|A|$ where a mixed vortex-TS flow can exist lies below the curve C_1 of figure (8). Outside this region only plane Poiseuille flow is possible. Hence at Taylor numbers greater than 32, finite amplitude vortices can exist only in the presence of TS waves. Thus, in this regime the TS waves are responsible for the existence of any vortices in the flow.

Our results therefore suggest that experimentally there can be a significant difference in the response of the flow to a TS wave dependent on the wall curvature. At relatively small curvatures, small amplitude TS waves will equilibrate to a size fixed by its frequency. If that frequency is decreased, then the TS wave size increases until the vortex flow is destroyed. At higher curvatures no vortex flow (with the given prescribed wavelength presumably introduced by wall roughness or turbulence in an experiment) can exist unless a TS wave is also present. If the TS amplitude is decreased, the vortices are again destroyed. Hence, at any Taylor number a sufficiently large TS wave introduced into the flow will destroy any vortex flow.

It is of interest to note that the calculations suggest that no mixed vortex-TS state can persist at Taylor numbers below the linear critical value of $6\sqrt{3}$. The work of Hall & Smith (**13,14**) suggests that the vortex-TS interactions at larger vortex wavelengths can, even without curvature, lead to singularities developing simultaneously in both time and the spanwise co-ordinate. Our results suggest that the transfer of energy is possible on smaller scales and so the results of Hall & Smith do not continue indefinitely.

REFERENCES

1). W.D. Harvey & J. Pride, *AIAA Jl. Paper No. 82-0567* (1967).

2). P. Hall & W.D. Lakin, *Proc. R. Soc. Lond. A.* **415**:421 (1988).

3). A.H. Nayfeh, *J. Fluid Mech.* **107**:441 (1981).

4). P. Hall, *J. Fluid Mech.* **130**:41 (1983).

5). P. Hall, *J. Fluid Mech.* **124**:475 (1982).

6). P. Hall, *J. Fluid Mech.* In the press.

7). M. Malik, *AIAA Jl. Paper No. 86-1129* (1986).

8). J. Bennett & P. Hall, *J. Fluid Mech.* **186**:445 (1988).

9). F.T. Smith, *Proc. R. Soc. Lond. A.* **366**:91 (1979).

10). F.T. Smith, *Proc. R. Soc. Lond. A.* **368**:573 (1979).

11). J. Bennett, P. Hall & F.T. Smith, *To appear as an ICASE report* (1988).

12). P. Hall & F.T. Smith, *Proc. R. Soc. Lond. A.* **417**:255 (1988).

13). P. Hall & F.T. Smith, *To appear in J. Fluid Mech.* (1988).

14). P. Hall & F.T. Smith, *To appear in Mathematika* (1988).

15). Q.I. Daudpota, P. Hall & T. Zang, *To appear in J. Fluid Mech.* (1988).

16). W.R. Dean, *Proc. R. Soc. Lond. A.* **121**:402 (1928).

17). S.P. Hastings & J.B. McLeod, *Arch. Rat. Mech. and Anal.* **73**:31 (1978).

18). P. Hall, *J. Inst. Mat. Applics.* **29**:173 (1982).

19). M. Abramowitz & I.A. Stegun, *A handbook of mathematical functions, Dover, New York* (1972).

FIGURE CAPTIONS

Fig. (1). Positions of the lower and upper shear layers y_1, y_2 as a function of the Taylor number T_0.

Fig. (2). Dependence of the Taylor number T_0 on the pressure gradient D when the constraint of constant non-dimensional mass flux is imposed.

Fig. (3). Graph to show the dimensional mass flow rate as a function of the pressure drop in a realistic experiment. In the absence of vortices the relationship is linear (solid line). When vortices are present, one of the broken lines is followed (which of the curves is determined by the physical parameters of the apparatus) which show that as the mass flux slowly rises an increasingly large change in pressure gradient is required. Indeed, for any particular case the possible values for mass flow rate are bounded above and these bounds are indicated for the lower two curves in the figure.

Fig. (4). Graph of the pressure gradient D against Taylor number T_0 for a variety of values of $\hat{\lambda} = 8\alpha^2|A|^2/T_0$. The lines (1)-(10) each follow a path of constant $\hat{\lambda}$ up to the point where $T_0 D^2 = 1000$, and are given by (1) $\hat{\lambda}$=10^{-4}, (2) $\hat{\lambda}$= 10^{-2}, (3) 5×10^{-2}, (4) 0.1, (5) 0.2, (6) 0.3, (7) 0.4, (8) 0.5, (9) 0.8 & (10) 1.0. The dotted line $D = 2$ corresponds to the problem where no vortices are present and the flow is plane Poiseuille with a linear TS wave of arbitrary amplitude imposed.

Fig. (5). The development of two of the curves of fig. (4) for larger values of T_0. (i) $\hat{\lambda} = 0.01$ (curve (2) in fig. (4)), (ii) $\hat{\lambda} = 0.2$ (curve (5) in fig. (4)).

Fig. (6). Position of the shear layers y_1 and y_2 as functions of the Taylor number T_0 for the cases (i) $\hat{\lambda} = 0.01$, (ii) $\hat{\lambda} = 0.2$. The positions of y_1 which correspond to the Painlevé shear layer problem lie between the crosses marked on the lower curves.

Fig. (7). Mean flow velocity profiles for $\hat{\lambda} = 0.2$ when (i) $T_0 = 19.98$, (ii) $T_0 = 23.52$ & $T_0 = 26.61$. The dotted lines represent the positions of the shear layers.

Fig. (8). Constant frequency curves in Taylor number/amplitude space. The values on each line are (i) $\Omega = 10$, (ii) $\Omega = 25$, (iii) $\Omega = 36.5$, (iv) $\Omega = 1200$ & (v) $\Omega = 1600$. The dotted line (C_1) corresponds to the limiting case $\Omega \longrightarrow 7.4016$.

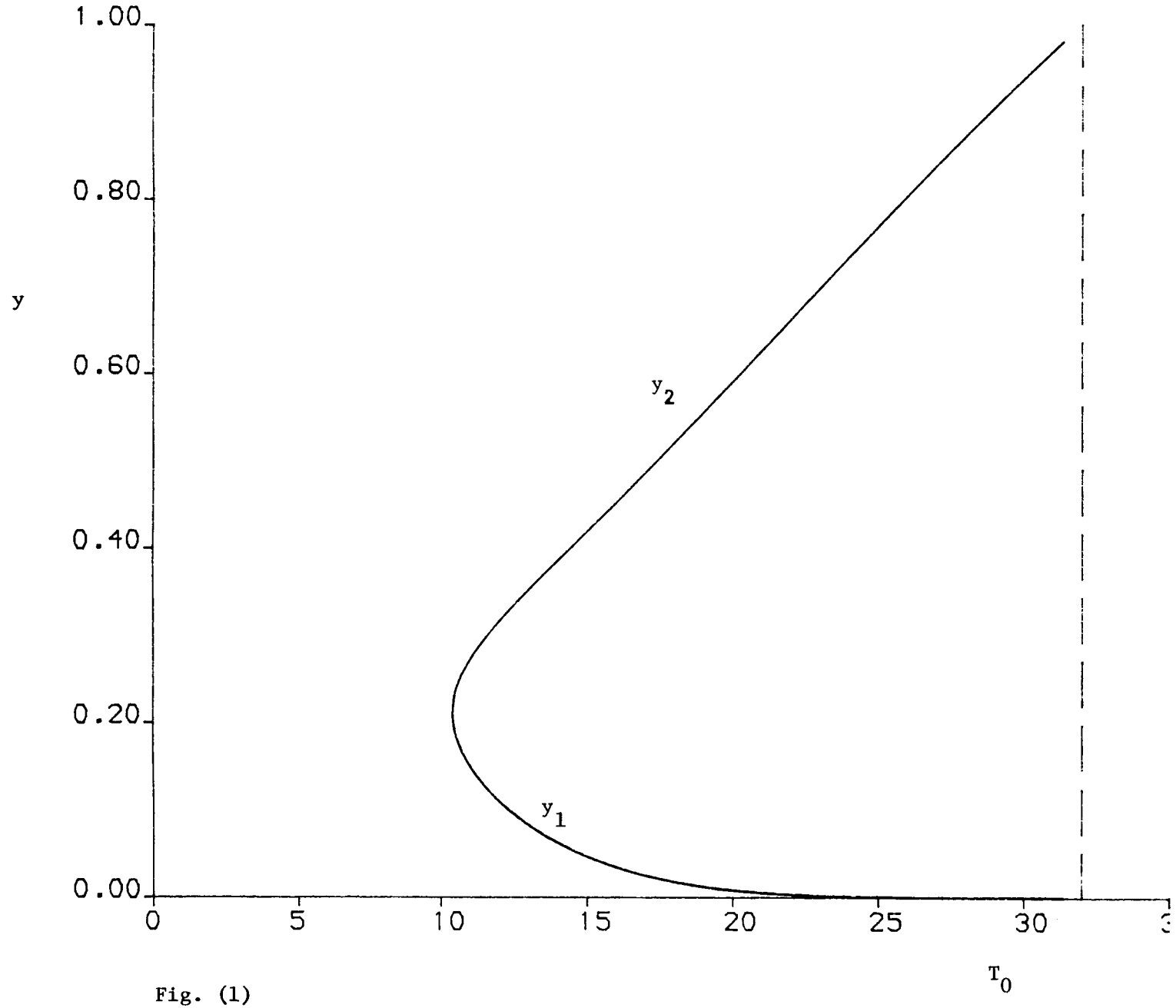

Fig. (1)

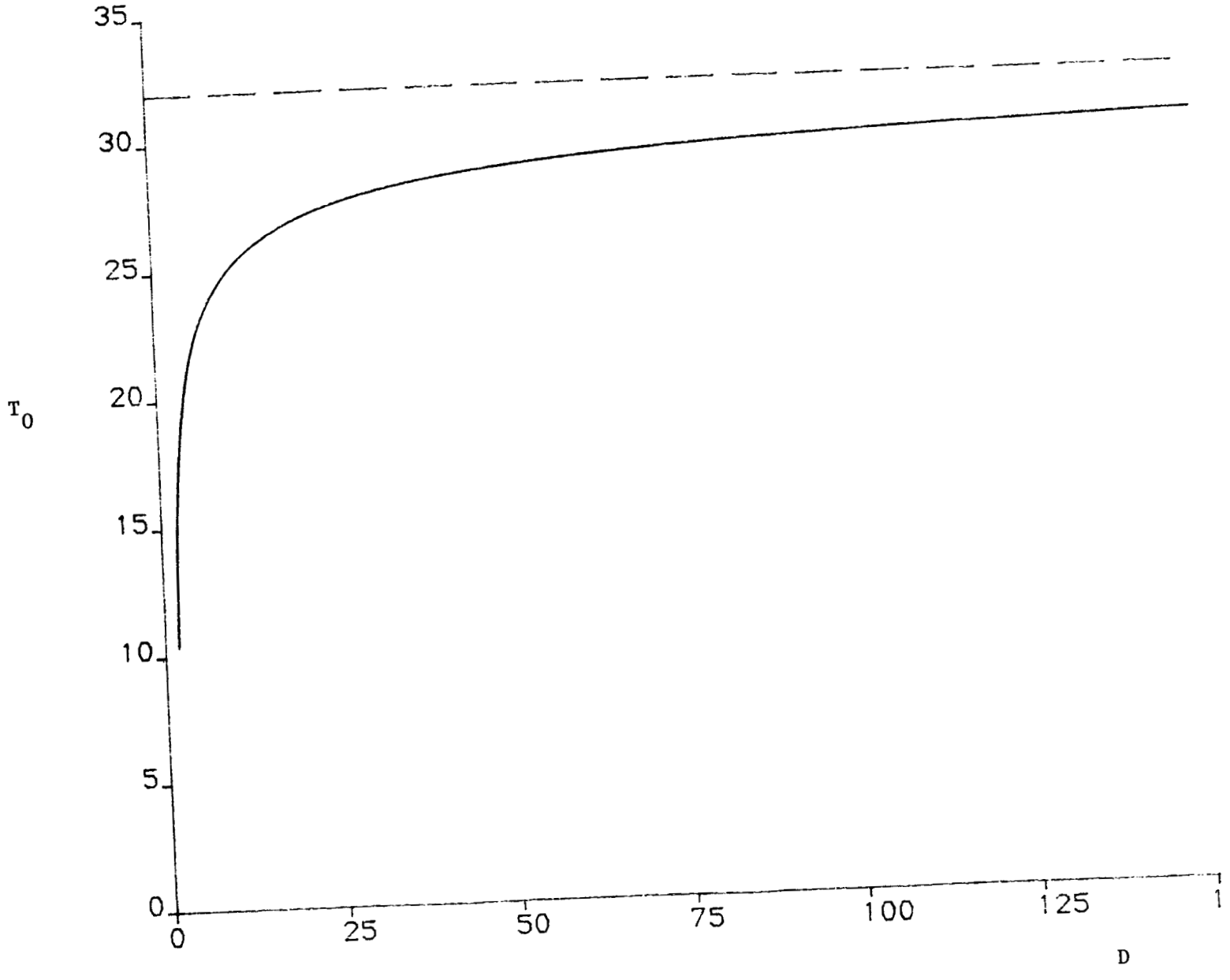

Fig. (2)

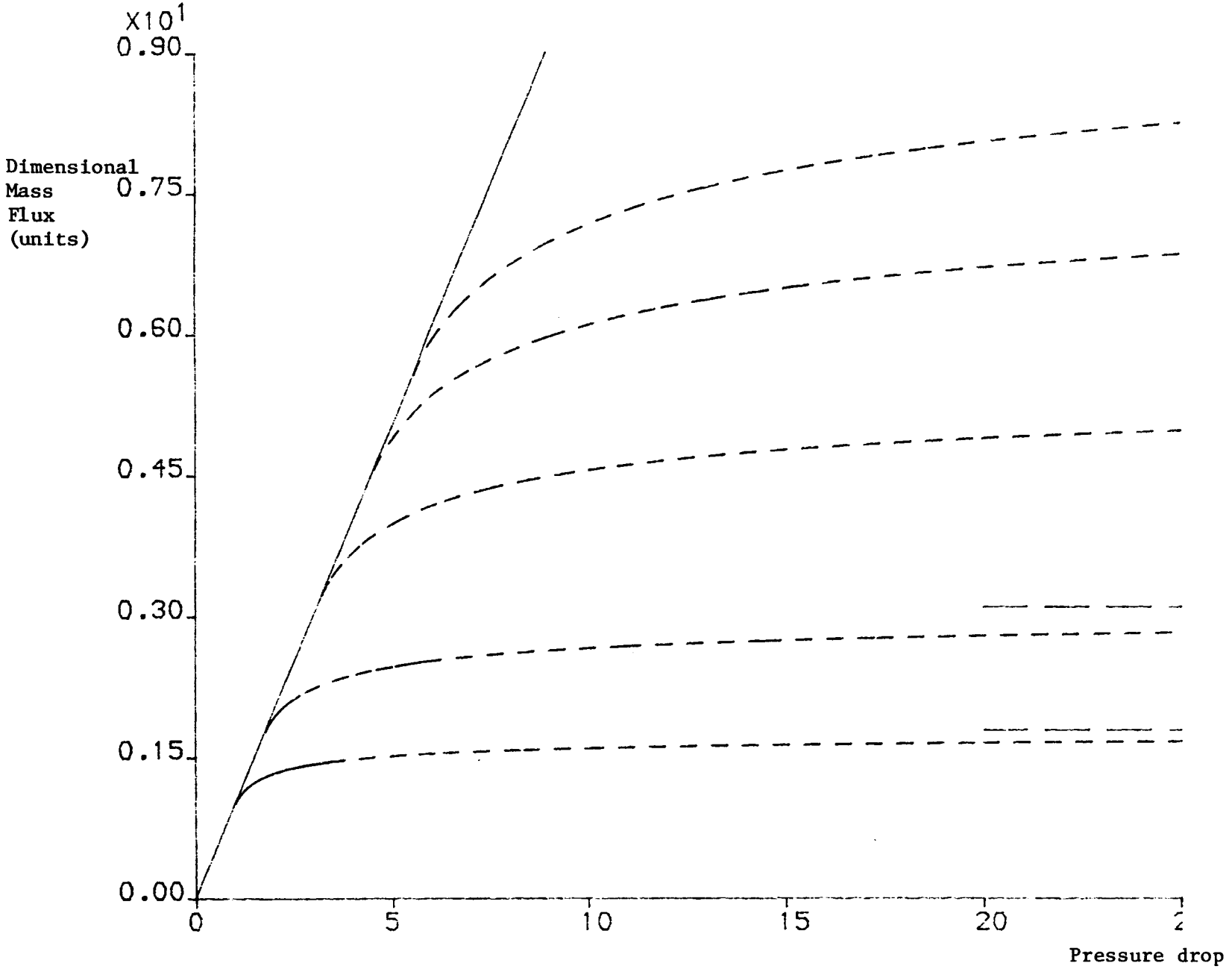
X10^1
0.90
0.75
0.60
0.45
0.30
0.15
0.00
Dimensional
Mass
Flux
(units)
0
5
10
15
20
Pressure drop

Fig. (3)

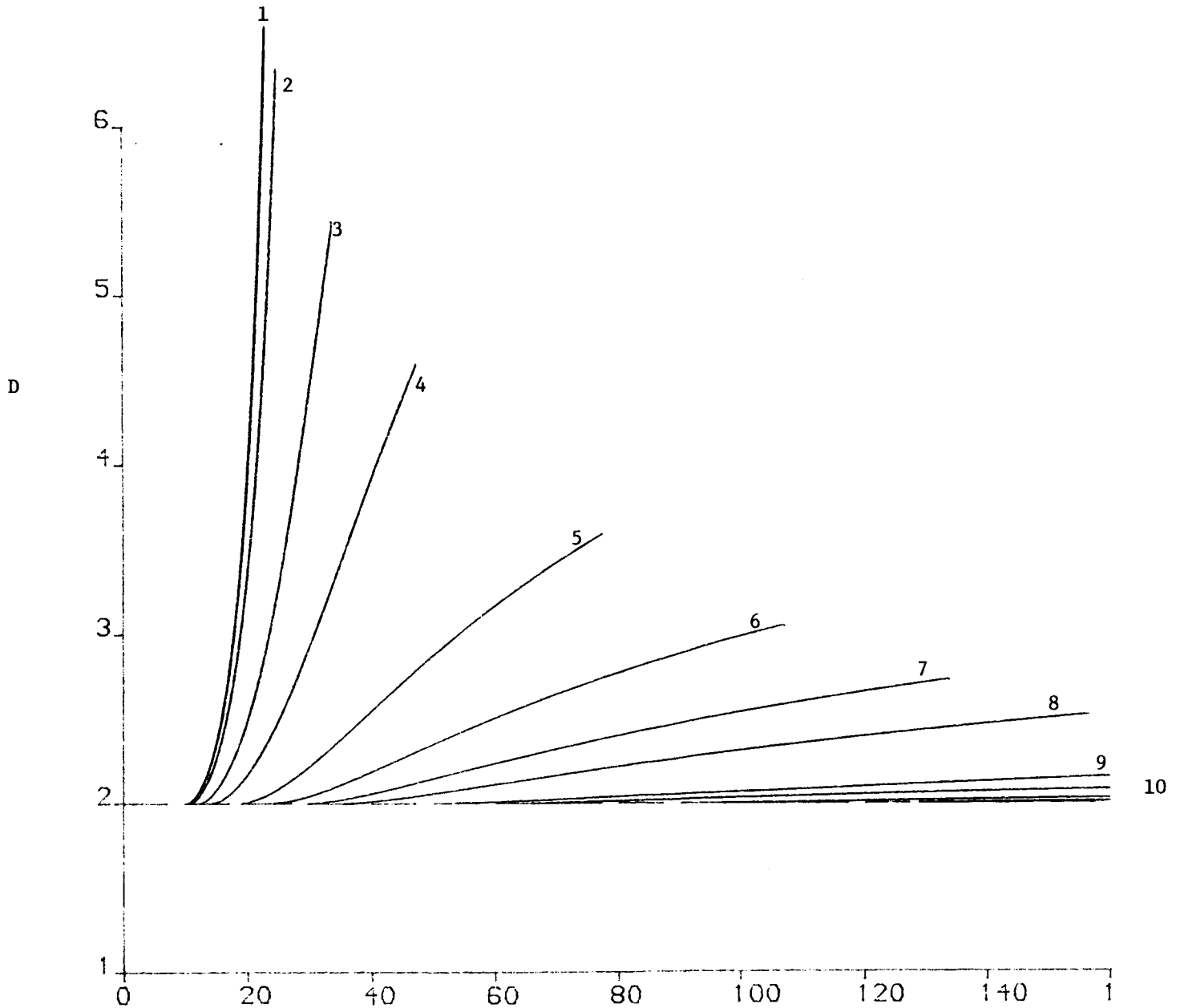

Fig. (4)

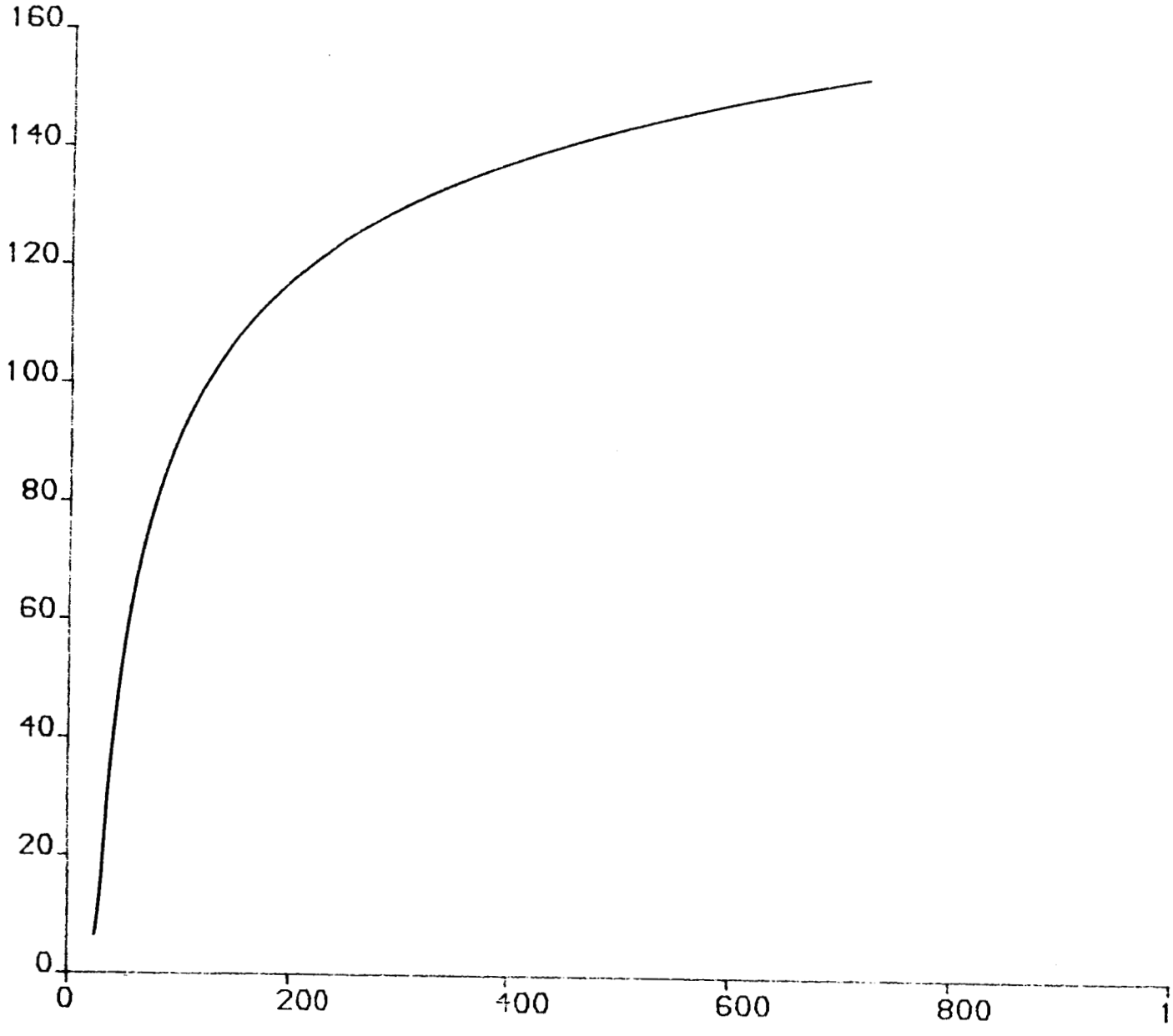

Fig. (5)(i)

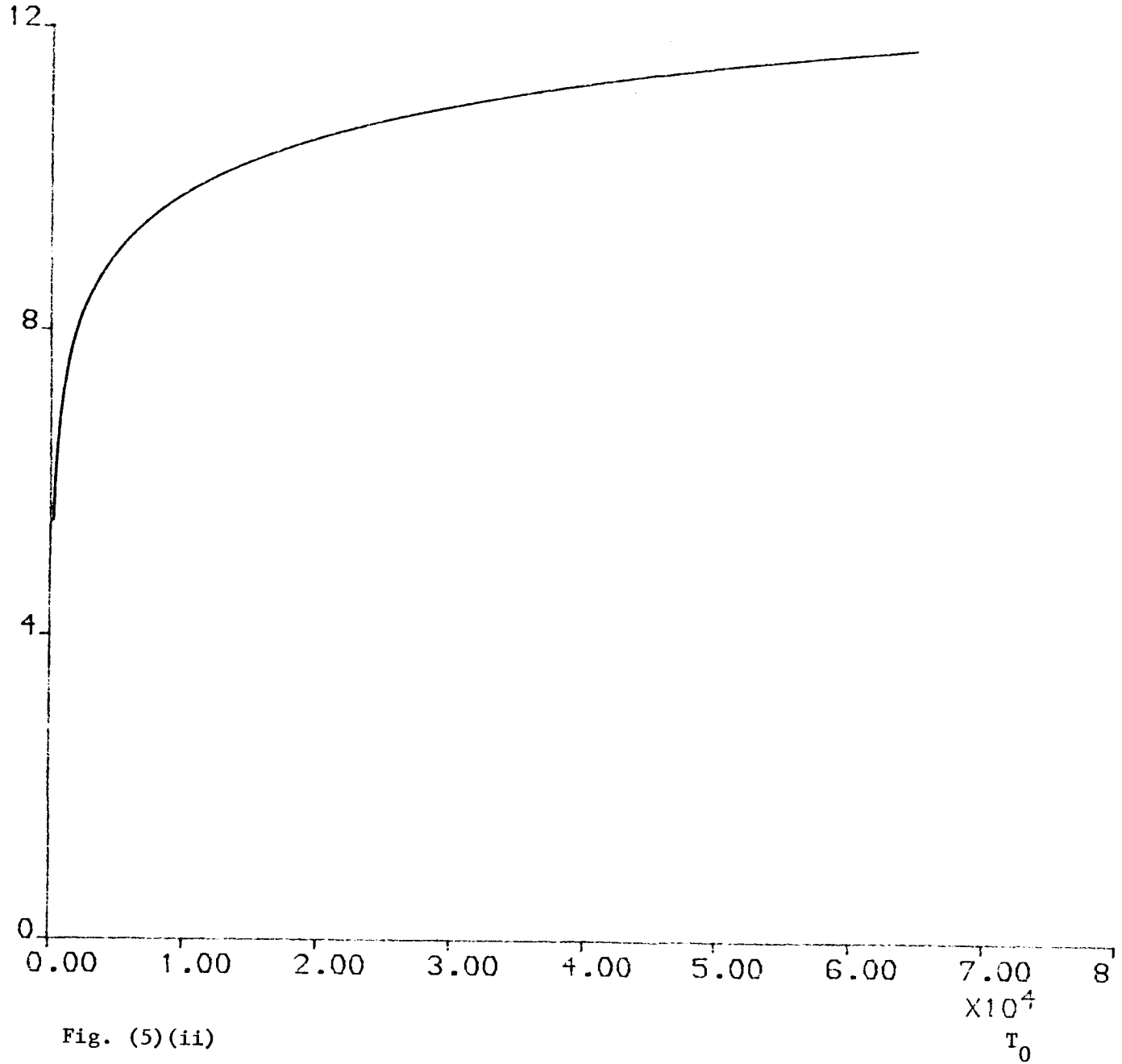

Fig. (5)(ii)

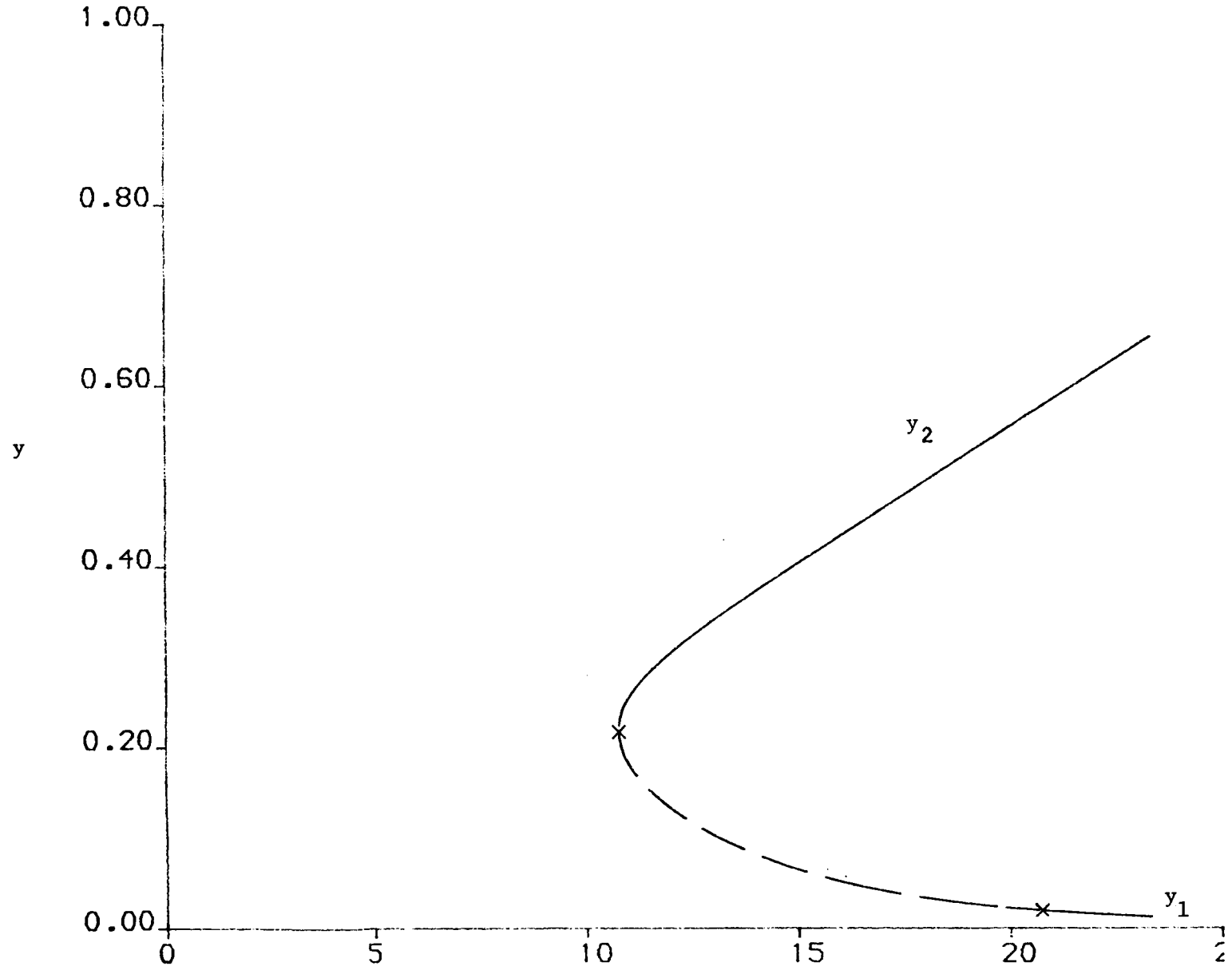

Fig. (6)(i)

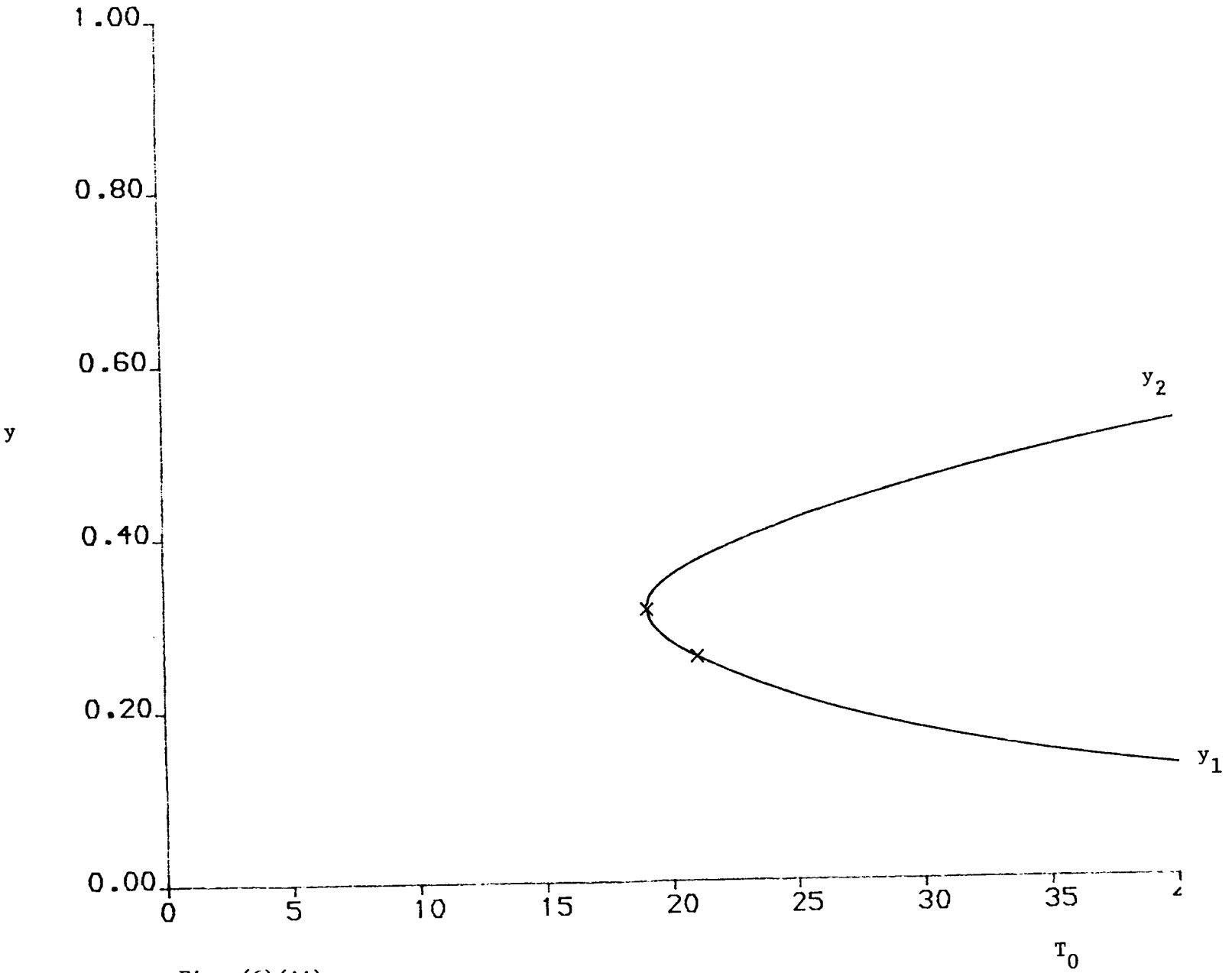

Fig. (6)(ii)

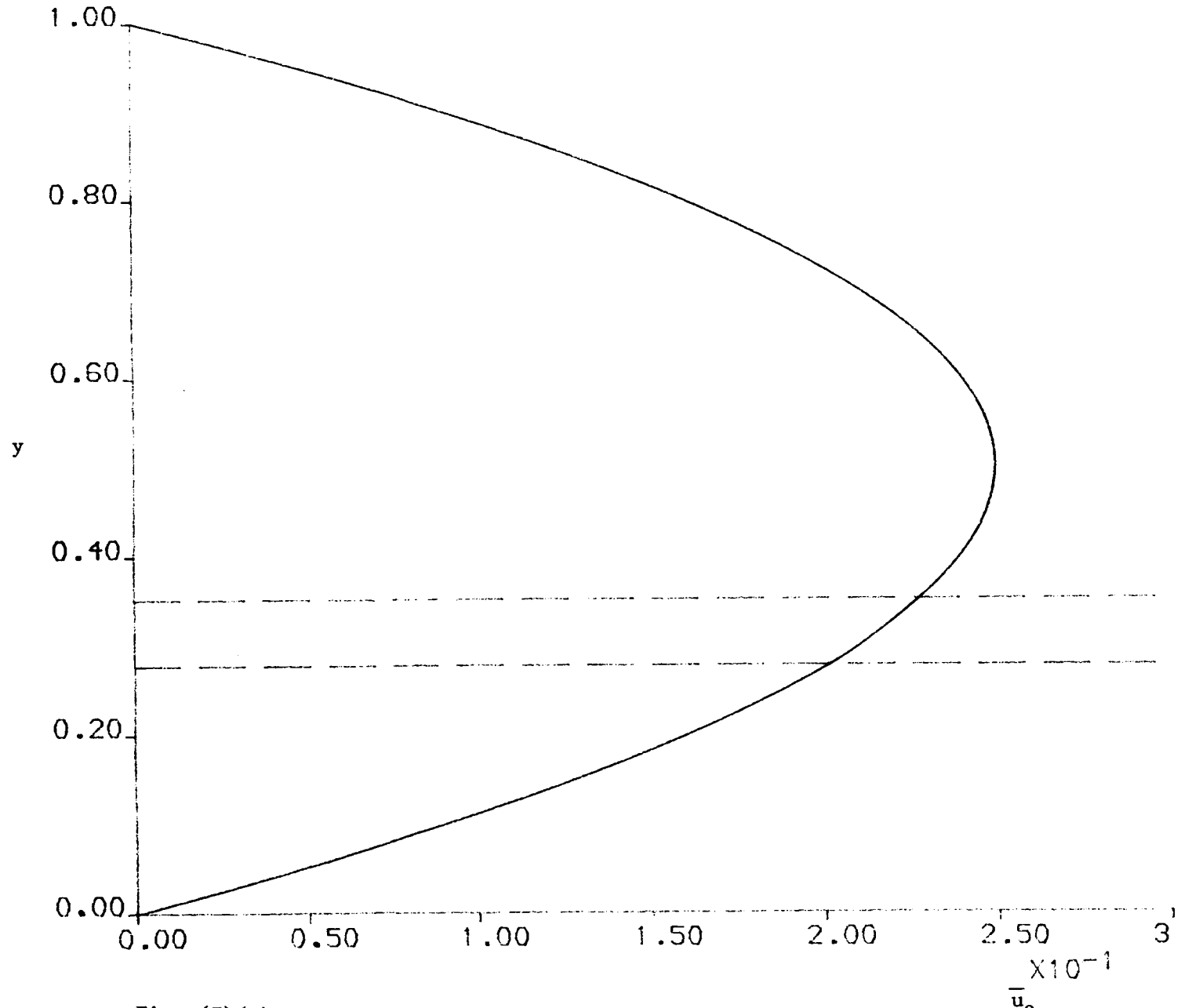

Fig. (7)(i)

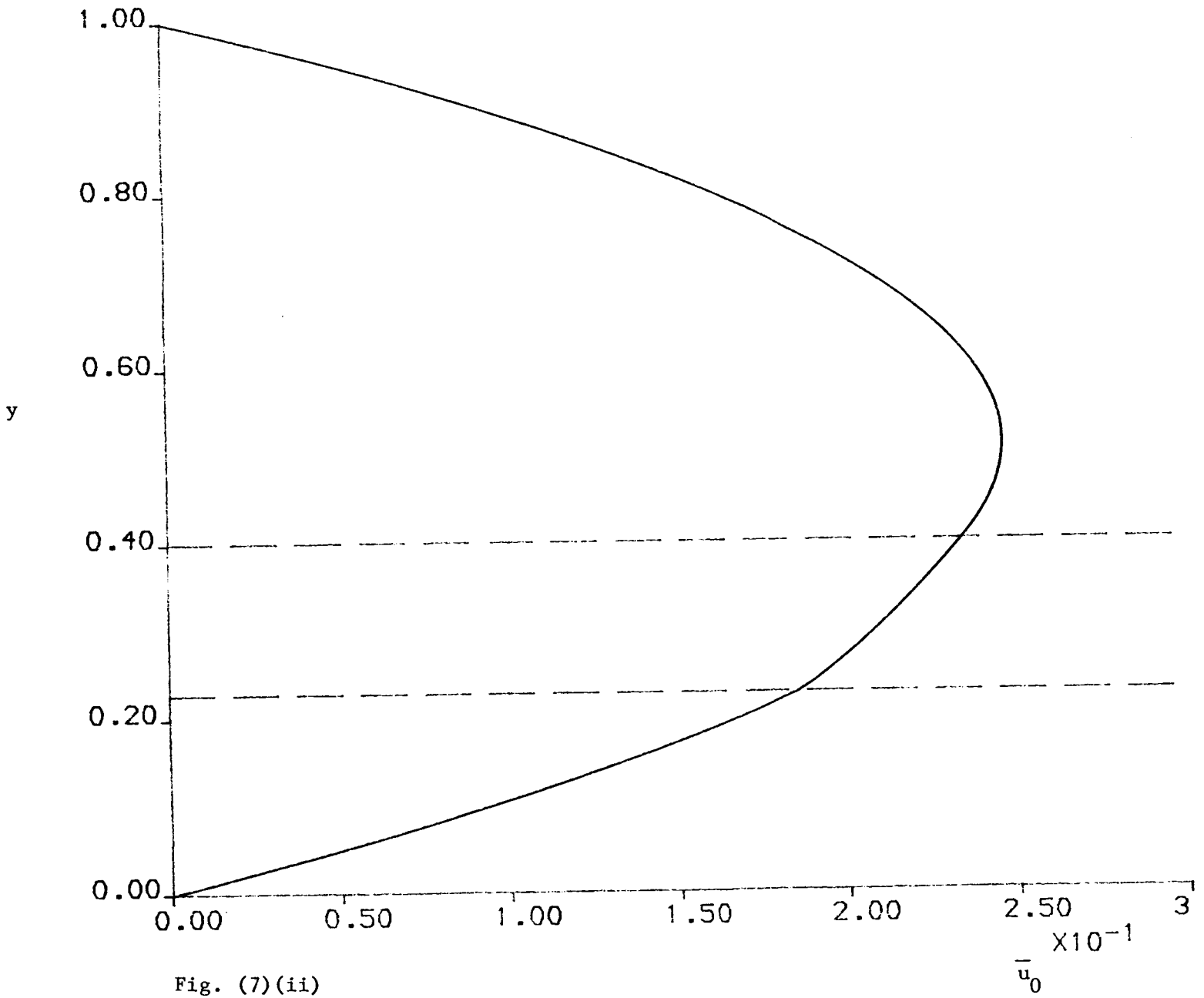

Fig. (7)(ii)

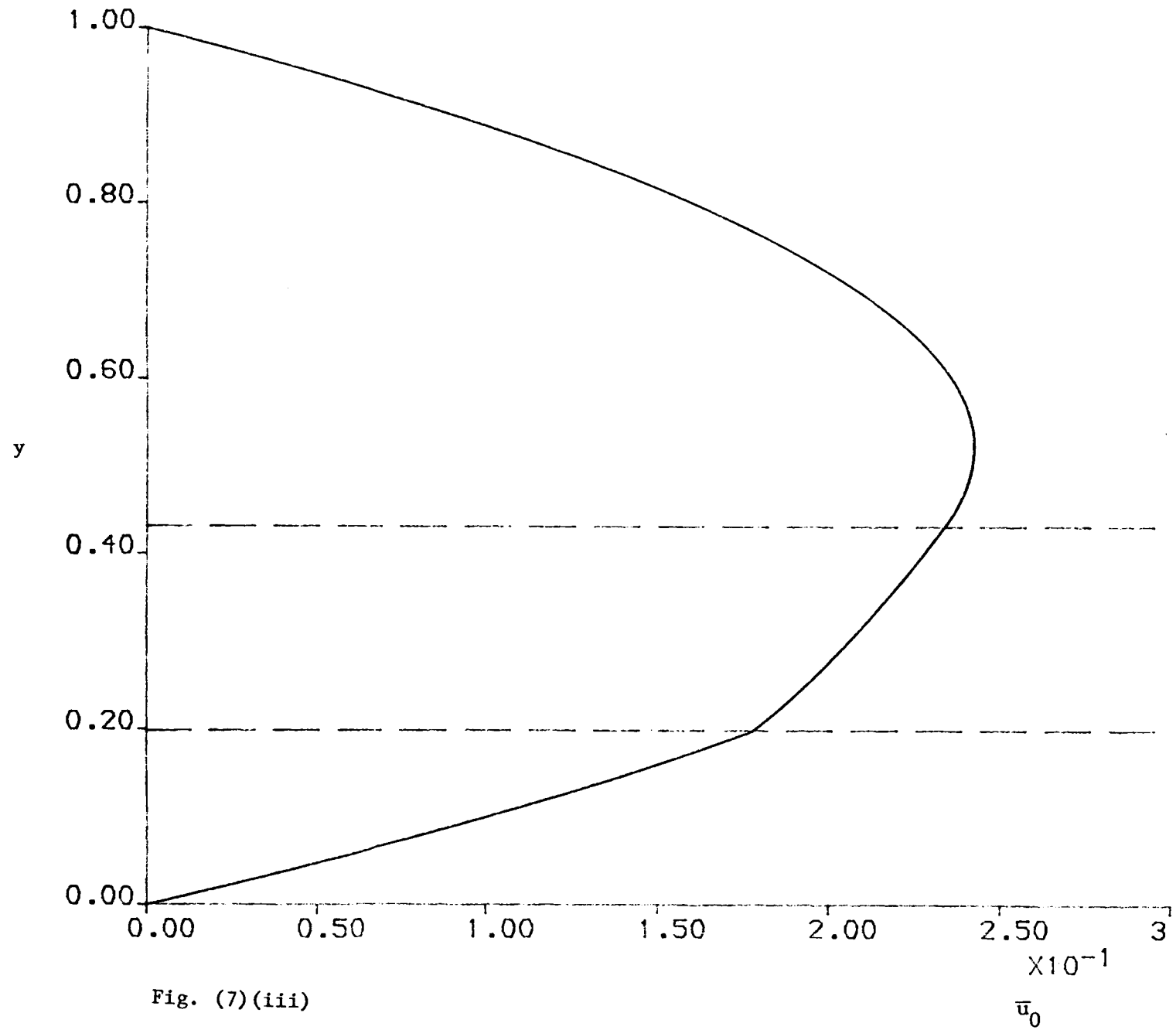

Fig. (7)(iii)

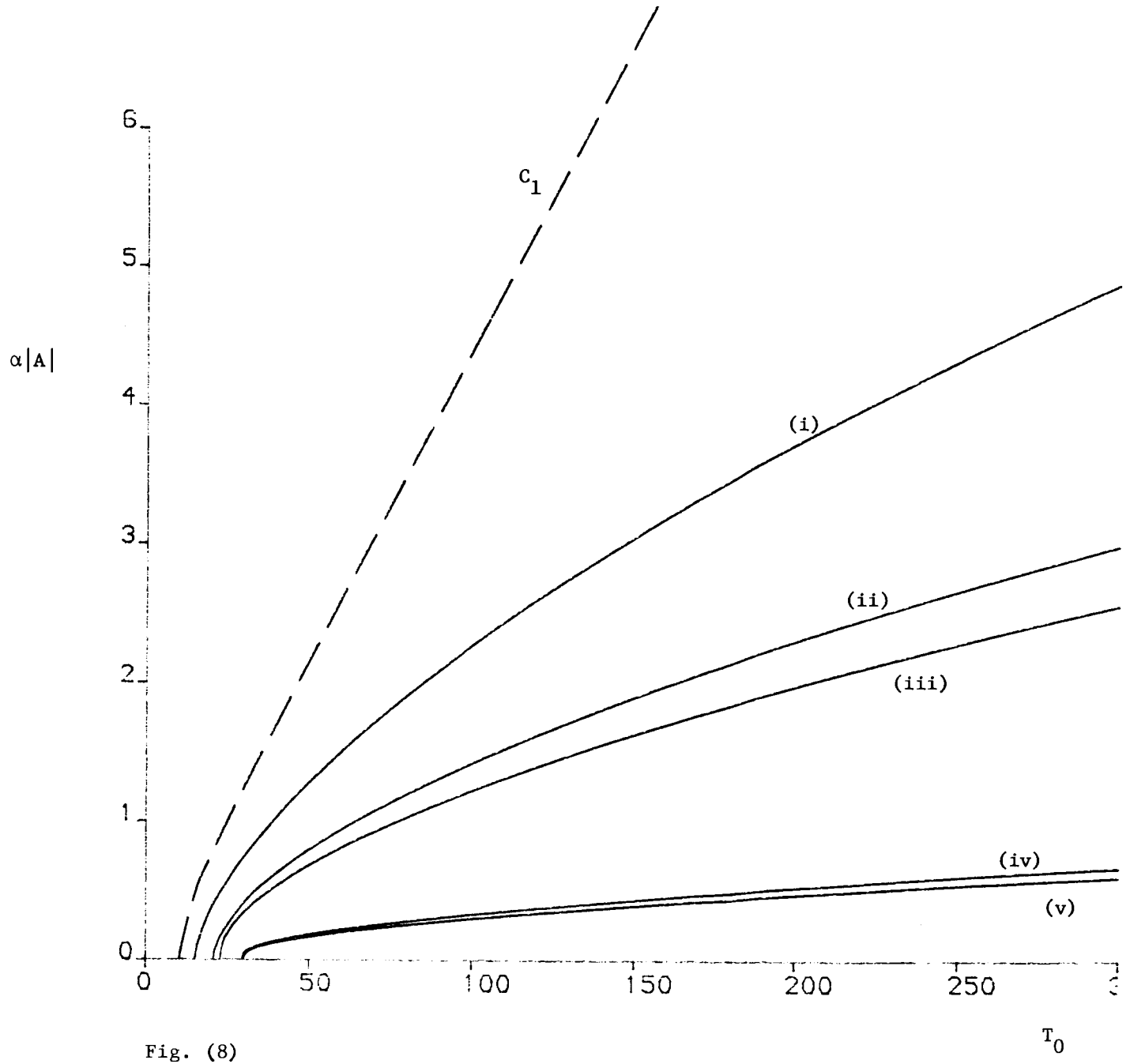

Fig. (8)

NASA National Aeronautics and Space Administration

Report Documentation Page

1. Report No.	2. Government Accession No.	3. Recipient's Catalog No.
NASA CR-181690 ICASE Report No. 88-43		

4. Title and Subtitle	5. Report Date
ON THE GENERATION OF MEAN FLOWS BY THE INTERACTION OF GÖRTLER VORTICES AND TOLLMIEN-SCHLICHTING WAVES IN CURVED CHANNEL FLOWS	July 1988
	6. Performing Organization Code

7. Author(s)	8. Performing Organization Report No.
Andrew P. Bassom and Philip Hall	88-43
	10. Work Unit No. 505-90-21-01

9. Performing Organization Name and Address	11. Contract or Grant No.
Institute for Computer Applications in Science and Engineering Mail Stop 132C, NASA Langley Research Center Hampton, VA 23665-5225	NAS1-18107, NAS1-18605
	13. Type of Report and Period Covered Contractor Report

12. Sponsoring Agency Name and Address	14. Sponsoring Agency Code
National Aeronautics and Space Administration Langley Research Center Hampton, VA 23665-5225	

15. Supplementary Notes

Langley Technical Monitor:
Richard W. Barnwell

Final Report

Submitted to Studies in Applied Maths.

16. Abstract

There are many fluid flows where the onset of transition can be caused by different instability mechanisms which compete in the nonlinear regime. Here the interaction of a centrifugal instability mechanism with the viscous mechanism which causes Tollmien-Schlichting waves is discussed. The interaction between these modes can be strong enough to drive the mean state; here the interaction is investigated in the context of curved channel flows so as to avoid difficulties associated with boundary layer growth. Essentially it is found that the mean state adjusts itself so that any modes present are neutrally stable even at finite amplitude. In the first instance, the mean state driven by a vortex of short wavelength in the absence of a Tollmien-Schlichting wave is considered. It is shown that for a given channel curvature and vortex wavelength there is an upper limit to the mass flow rate which the channel can support as the pressure gradient is increased. When Tollmien-Schlichting waves are present then the nonlinear differential equation to determine the mean state is modified. At sufficiently high Tollmien-Schlichting amplitudes it is found that the vortex flows are destroyed, but there is a range of amplitudes where a fully nonlinear mixed vortex-wave state exists and indeed drives a mean state having little similarity with the flow which occurs without the instability modes. The vortex and Tollmien-Schlichting wave structure in the nonlinear regime has viscous wall layers and internal shear layers; the thickness of the internal layers is found to be a function of the Tollmien-Schlichting wave amplitude.

17. Key Words (Suggested by Author(s))	18. Distribution Statement
vortices, Tollmien-Schlichting waves	01 - Aeronautics (General) Unclassified - unlimited

19. Security Classif. (of this report)	20. Security Classif. (of this page)	21. No. of pages	22. Price
Unclassified	Unclassified	40	A03